Original article

The new 5- or 6-azapyrimidine and cyanuric acid derivatives of L-ascorbic acid bearing the free C-5 hydroxy or C-4 amino group at the ethylenic spacer: CD-spectral absolute configuration determination and biological activity evaluations

K. Wittine [a], M. Stipković Babić [a], M. Košutić [a], M. Cetina [b,c], K. Rissanen [c], S. Kraljević Pavelić [d], A. Tomljenović Paravić [d], M. Sedić [e], K. Pavelić [d], M. Mintas [a,*]

[a] Department of Organic Chemistry, Faculty of Chemical Engineering and Technology, University of Zagreb, Marulićev trg 20, HR-10000 Zagreb, Croatia
[b] Department of Applied Chemistry, Faculty of Textile Technology, University of Zagreb, Prilaz baruna Filipovića 28a, HR-10000 Zagreb, Croatia
[c] Department of Chemistry, NanoScience Center, University of Jyväskylä, P.O. Box 35, FI-40014 Jyväskylä, Finland
[d] Department of Biotechnology, University of Rijeka, trg braće Mažuranića 10, 51000 Rijeka, Croatia
[e] Division of Molecular Medicine, Rudjer Bošković Institute, Bijenička cesta 54, HR-10000 Zagreb, Croatia

ARTICLE INFO

ABSTRACT

We report on the synthesis of the novel types of cytosine and 5-azacytosine (**1**–**9**), uracil and 6-azauracil (**13**–**18**) and cyanuric acid (**19**–**22**) derivatives of L-ascorbic acid, and on their cytostatic activity evaluation in human malignant tumour cell lines vs. their cytotoxic effects on human normal fibroblasts (WI38). The CD spectra analysis revealed that cytosine (**5** and **6**), uracil (**14**–**16**), 6-azauracil (**17**) and cyanuric acid (**21**) derivatives of L-ascorbic acid bearing free amino group at ethylenic spacer existed as a racemic mixture of enantiomers, whereas L-ascorbic derivatives containing the C-5 substituted hydroxy group at the ethylenic spacer were obtained in (4R, 5S) enantiomeric form. The stereochemistry of 6-azauracil derivative of L-ascorbic acid (**13**) was confirmed by X-ray crystal structure analysis. The molecules are self-assembled by one N—H···O hydrogen bond, two C—H···O hydrogen bonds and two C—H···π interactions into three-dimensional framework. Cytostatic activity evaluation indicated that compounds did not show distinctive antiproliferative effects on tested cell line panel. However, the cytosine derivative of L-ascorbic acid (**1**) containing the C4-C5 double bond conjugated with the lactone moiety produced rather marked growth inhibitory effect on hepatocellular carcinoma (HepG2), metastatic breast epithelial carcinoma (MCF-7) and cervical carcinoma (HeLa) cell lines at micromolar concentrations, but also exerted strong cytostatic effect on WI38. 5-Azacytosine derivative of L-ascorbic acid (**2**) with a double bond at the C4—C5 conjugated with the lactone moiety displayed potent antitumour activity against tested tumour cell lines with meanIC$_{50}$ values ranging from 0.92 to 5.91 μM. However, this compound also exhibited pronounced cytotoxicity towards WI38. Flow cytometric analysis of the cell cycle revealed that compound **2** triggers S phase arrest, which clearly demonstrates its interference with DNA replication, a key event of cell proliferation. Marked anticancer efficacy of compound **2** supports further in vivo investigation into its possible clinical utility.

© 2011 Elsevier Masson SAS. All rights reserved.

1. Introduction

Nucleoside analogues represent a valuable source that contributes significantly to the arsenal of chemotherapeutic agents against viruses and cancer. In recent years, a number of five-membered cytosine nucleoside analogues, such as 1-(2-deoxy-2-methylene-β-D-erythro-pentofuranosyl) cytosine (DMDC) [1], 2′-deoxy-2′,2′-difluorocytidine (gemcitabine) [2], and 1-(2-C-cyano-2-deoxy-β-D-arabino-pentofuranosyl) cytosine (CNDAC) [3], have been developed as potent antitumour agents effective not only in leukemias and lymphomas, but also in a wide variety of solid tumours in vitro and in vivo. L-ascorbic acid (vitamin C), a water-soluble vitamin essential for hundreds of vital metabolic reactions, and its isomers have garnered great attention as anticancer agents, although the mechanisms underlying their antitumour activity have not been fully elucidated. In spite of the fact that it cannot be produced by the human body, vitamin C is integral to the formation of collagen, connective tissue, and immune system factors, and also serves important anti-inflammatory and

* Corresponding author. Tel.: +385 1 4597 214; fax: +385 1 4597 250.
E-mail address: mladen.mintas@fkit.hr (M. Mintas).

antioxidant functions. Cameron and Pauling believed that L-ascorbic acid combats cancer by promoting collagen synthesis that prevents tumours from invading other tissues [4]. However, researchers now believe that L-ascorbic acid fights cancer by neutralizing free radicals before they can damage DNA and initiate tumour growth, and/or may act as a pro-oxidant helping body's own free radicals to destroy tumours in their early stages [5–7]. For example, a mixture of L-ascorbic acid and cupric sulfate significantly inhibited human mammary tumour growth in mice when administered orally [8]. A number of ascorbic acid isomers/derivatives have been synthesized and tested on tumour cell lines so far. It was shown that L-ascorbic acid modulates the *in vitro* growth of colonies of human and mouse myeloma progenitor/stem cells and leukemic colony-forming cells from bone marrow of patients with acute myelocytic leukemia [9]. Furthermore, L-Ascorbic acid and its derivatives were cytotoxic and suppressed the growth of malignant leukemia cell line P388D1 *in vivo* in the following order of potency: 6-deoxy = dihydroxy-γ-crotonolactone ($-Cl$, $-Br$, $-NH_2$) > L-ascorbic acid and its stereo-isomer D-ascorbic acid, D-isoascorbic acid and dehydroascorbic acid > 6-substituted ($-PO_4$, $-SO_4$, -palmitate, -stearate) > 2,6-disubstituted (dipalmitate) > 2-substituted ($-PO_4$, $-SO_4$, *O*-Me, *O*-octadecyl) > dihydroxy-γ-butyrolactone [10–12]).

Several studies have provided evidence for cytotoxicity of L-ascorbic acid in some human tumour cells, neuroblastoma [13], osteosarcoma and retinoblastoma [14]. Substitution at 2-, 6- and 2,6-positions in L-ascorbic acid modulates its cytotoxic potential against malignant cells. Furthermore, ascorbate-6-palmitate and ascorbate-6-stearate are more potent growth inhibitors of murine leukemia cells than ascorbate 2-phosphate, ascorbate-6-phosphate and ascorbate-6-sulphate [15]. In addition, ascorbyl palmitate and ascorbyl stearate have attracted considerable interest in view of their potential use as anticancer compounds, whose lipophilic nature allows them to easily traverse cell membranes and blood—brain barrier [16]. L-Ascorbic acid and ascorbyl esters were shown to inhibit the proliferation of mouse glioma and human brain tumour cells, glioma (U-373) and glioblastoma (T98G) cells, and renal carcinoma cells [17–19]. The role of sodium-L-ascorbate in angiogenesis was ascertained by the study demonstrating its inhibitory effect on the formation of vessel-like tubular structures of endothelial cells cultured on Matrigel [20].

Related to our previous findings that some pyrimidine and purine derivatives of 4,5-didehydro-5,6-dideoxy-L-ascorbic acid posses pronounced cytostatic activity against some malignant tumour cell lines [21–23], we have synthesized a series of novel pyrimidine derivatives containing *C*4-*C*5 double bond conjugated with the lactone moiety (**1–4**, **13**, **19**, **20**), and their congeners bearing free hydroxy group at *C*-5 of the ethylenic spacer (**7–9**, **18**, **22**), as well as pyrimidine derivatives (**5**, **6**, **14–17**, **21**) with the amino group at the *C*-4 of the lactone moiety (Fig. 1). Besides synthesis, the present study provides information on their cytostatic activities in different human tumour cell lines and cytotoxic effects on human normal fibroblasts.

2. Results and discussion

2.1. Chemistry

Cytosine and 5-azacytosine derivatives of L-ascorbic acid (**1–9**) (Scheme 1) were prepared by the reaction of the silylated cytosine bases (BzCt: benzoylated cytosine and 5-AzaC: 5-azacytosine) with 5,6-di-*O*-acetyl-2,3-di-*O*-benzyl-L-ascorbic acid (**dAdBA**) or epoxy-2,3-di-*O*-benzyl-L-ascorbic acid (**EdBA**) under Vorbrüggen reaction conditions.

Silylated *N*⁴-benzoylcytosine was reacted with 5,6-di-*O*-acetyl-2,3-di-*O*-benzyl-L-ascorbic acid (**dAdBA**) to give cytosine derivative **1** as a mixture of (*Z*)- and (*E*)-isomers. Crystallization of this diastereomeric mixture from ethanol gave pure (*Z*)-isomer of **1**, which was

then subjected to either debenzylation with boron-trichloride to give **3**, or to ammonolysis with ammonium in methanol to yield compound **5**. Besides removing the *N*⁴-benzoyl protecting group, ammonolysis created in this reaction a new chiral stereocenter with the amino group at the *C*-4 position of the lactone moiety (**5**). 5-Azacytosine (**5-AzaC**) was silylated in an analogous way by using 1,1,1,3,3,3-hexamethyldisilazane (**HMDS**) and catalytic amount of ammonium-sulphate. The resulted silylated base was reacted *in situ* with **dAdBA** to give **2** with the assistance of the Friedel-Crafts catalyst, trimethylsilyltrifluoromethane sulphonate (TMSOTf). Debenzylation with 1 M boron-trichloride in dichloromethane yielded **4** with free enolic hydroxyl group at *C*-2 of L-ascorbic acid moiety. Reaction of **2** with ammonia in methanol/dioxane mixture gave compound **6** bearing the amino group at the *C*-4 of L-ascorbic acid lactone moiety.

Reaction of silylated *N*⁴-benzoylcytosine with the 4-(5,6)-epoxy-2,3-di-*O*-benzyl-L-ascorbic acid (**EdBA**) gave cytosine L-ascorbic acid derivative (**7**) bearing the free hydroxy group at the *C*-5 position of the ethylenic spacer. Analogous reaction of 5-aza-cytosine with **EdBA** gave L-ascorbic acid derivative with the free hydroxyl group at the *C*-5 of the ethylenic spacer (**8**). Subsequent removal of *N*⁴-benzoyl protecting group in **7** with methanolic ammonia gave **9** containing free hydroxy group at the *C*-5 of the ethylenic spacer (Scheme 1).

Pyrimidine derivatives of 4,5-didehydro-5,6-dideoxy-L-ascorbic acid (**10–12**) were prepared by condensation of uracil, 5-fluoro-uracil, thymine and 6-azauracil with 5,6-di-*O*-acetyl-2,3-di-*O*-benzyl-L-ascorbic acid (**dAdBA**) [23]. Related 6-azauracil derivative of L-ascorbic acid (**13**) was synthesized in an analogous manner. Ammonolysis of compounds **10–13** gave uracil (**14**), 5-fluorouracil (**15**), thymine (**16**) and 6-azauracil (**17**) derivatives of L-ascorbic acid with the amino group at the *C*-4 position of the lactone moiety. Reaction of silylated 6-azauracil with **EdBA** and TMSOTf furnished 6-azauracil derivative of L-ascorbic acid (**18**) bearing the free hydroxy group at the *C*-5 of the ethylenic spacer (Scheme 2).

In a similar manner, reaction of cyanuric acid (**CA**) and L-ascorbic acid derivatives (**dAdBA** and **EdBA**) afforded **19** and **22**. Reaction of **19** with methanolic ammonia yielded **21** with the free amino group at *C*-4, and with BCl₃ gave **20** with the free hydroxyl groups at the *C*2 and *C*3 positions of the lactone moiety (Scheme 3).

The structures of the novel 5- or 6-azapyrimidine and cyanuric acid derivatives of L-ascorbic acid were deduced from their ¹H NMR spectra (Table 1), as well as their ¹³C NMR and mass spectra.

The *Z*-configuration was deduced on the basis of comparison of coupling constants and chemical shifts in their ¹H and ¹³C NMR spectra with those of related L-ascorbic acid derivatives in which the *Z*- and *E*-configuration were assessed by the use of decoupling experiments and 2D NOESY and HMBC correlation experiments [21,22]. An unambiguous proof of the (*Z*)-configuration of 6-azauracil derivative of L-ascorbic acid (**13**) was obtained by its X-ray crystal structure analysis (*c.f.* Section 2.3).

2.2. UV and CD spectra

We analysed the circular dichroism (CD) spectra of L-ascorbic acid derivatives containing *C*-5 hydroxy group (**8**, Fig. 2A and **7**, Fig. 2B) or *C*-4 amino group (**5**, **6**, **14–17** and **21**) at the ethylenic spacer. This investigation was undertaken to deduce their absolute configurations and stereochemical course of condensation reactions (Schemes 1–3).

L-ascorbic acid moiety consists a γ-lactone ring in which enediol portion and the oxygen of the lactone moiety are conjugated to the carbonyl group. The UV spectra of enones are characterized by an intense absorption band (K-band) in the 215—250 nm region [24]. 5-Azacytosine derivative (**8**, Fig. 2A) exhibits UV-band at 205 nm (band II, $\epsilon = 32859$ mmol⁻¹ cm²) resulting from n → π*

A Cytosine and 5-azacytosine derivatives of L-ascorbic acid (**1-9**)
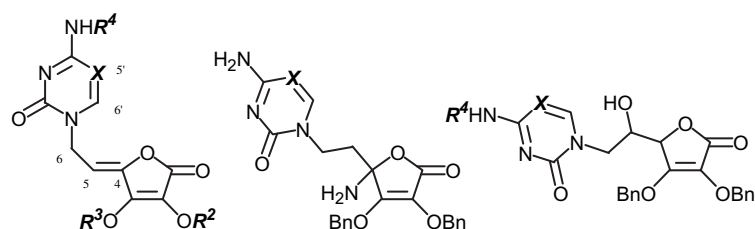
Comp.	R²	R³	R⁴	X
1	Bn	Bn	Bz	CH
2	Bn	Bn	H	N
3	H	H	H	CH
4	H	Bn	H	N

Comp.	X
5	CH
6	N

Comp.	R⁴	X
7	Bz	CH
8	H	N
9	H	CH

B Pyrimidine and 6-azauracil derivatives of L-ascorbic acid (**13-18**)
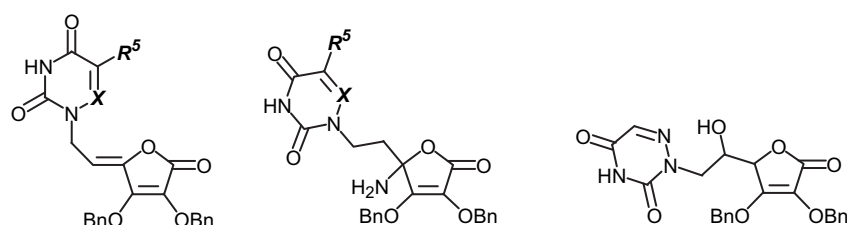
Comp.	R⁵	X
13	H	N

Comp.	R⁵	X
14	H	CH
15	F	CH
16	CH₃	CH
17	H	N

18

C Cyanuric acid derivatives of L-ascorbic acid (**19-22**)
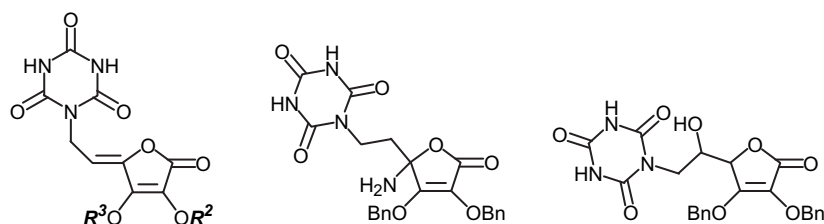
Comp.	R²	R³
19	Bn	Bn
20	H	H

21

22

Fig. 1. The novel pyrimidine derivatives of L-ascorbic acid (**1–9** and **13–22**).

transition and 239 nm (band I, $\epsilon = 14902$ mmol^{-1} cm^2) arising from $\pi \rightarrow \pi^*$ transition. The UV spectrum of N^4-benzoylcytosine derivative of L-ascorbic acid (**7**, Fig. 2B) has 3 electronic transitions. The weak band at 307 nm (band I, $\epsilon = 7121$ mmol^{-1} cm^2) belongs to the lowest energy transition. Empirically this band would be described as a carbonyl $n \rightarrow \pi^*$ transition but it actually has $\pi_{Ph} \rightarrow \pi_{CO}^*$ character [25]. The other two absorption maxima at 257 nm (band II, $\epsilon = 18858$ mmol^{-1}cm^2) and 205 nm (band III, $\epsilon = 31749$ mmol^{-1} cm^2) can be assigned to the $\pi \rightarrow \pi^*$ and $n \rightarrow \pi^*$ of the enone chromophore. They probably cover more then one electronic transition but can be assigned as designated above.

In the CD spectrum of **8** (Fig. 2A) the negative Cotton effect at 248 nm (band I, $\Delta\epsilon = -71.43$ mmol^{-1} cm^2) may be assigned to the $\pi \rightarrow \pi^*$ transition (K-band), while the one located at 209 nm (band II, $\Delta\epsilon = 59.60$ mmol^{-1} cm^2) can be attributed to the $n \rightarrow \pi^*$ transition (R-band). This assignment is in accord with that of structurally related cyclopentenone systems [24]. The lowest energy transition in the CD spectrum of **7** (Fig. 2B) gives rise to a negative Cotton effect around 304 nm (band I, $\Delta\epsilon = -10.96$ mmol^{-1} cm^2) which can be assigned to the $n \rightarrow \pi^*$ of the carbonyl group. This rather broad band appears usually between 320 and 350 nm but conjugation leads to a red shift of the $n \rightarrow \pi^*$ carbonyl band [25]. The $\pi_{Ph} \rightarrow \pi_{CO}^*$ excitation of the benzoyl

moiety is located at 264 nm (band II, $\Delta\epsilon = -8.81$ mmol^{-1} cm^2). A positive Cotton effect around 241 nm (band III, $\Delta\epsilon = 6.75$ mmol^{-1} cm^2) may be assigned to the $\pi \rightarrow \pi^*$ transition of the enone chromophore which considerably overlaps with the n $\rightarrow$ π^* of the benzamide chromophore [26] at 223 nm (band IV, $\Delta\epsilon = 5.86$ mmol^{-1} cm^2). This band is generally assigned to a ^{1}L$_a$ aromatic transition [27] although the intramolecular charge transfer transition has also been proposed as the origin of this band [28]. The band at 207 nm (band V, $\Delta\epsilon = 2.75$ mmol^{-1} cm^2) can be attributed to the n $\rightarrow$ π^* transition (R-band) but may also result from a transition within the aromatic ring.

We have previously assigned the 4*R*, 5*S* configuration to the 4-(5,6-epoxy) derivative of L-ascorbic acid on the basis of combined use of CD spectroscopy and X-ray crystal structure analysis [29]. Comparison of that spectrum with the CD spectra of *C*-5 hydroxy derivatives of L-ascorbic acid (**7** and **8**) shows that all three spectra are quite similar with negative Cotton effect trend but at different wavelengths due to difference in molecular structure or solvent effects. Thus, their configuration consequently has to be the same 4*R*, 5*S*. Ring opening of epoxy-L-ascorbic acid derivative occurs in a stereospecific manner giving rise to 5-azacytosine-(**8**) and N^4-benzoylcytosine derivative of L-ascorbic acid (**7**) with the same stereostructure at *C*-4 and *C*-5 of the ethylenic spacer. This is supported also by mechanistic consideration of the nucleophile attack of the epoxide derivative from the less hindered side.

Cytosine (**5** and **6**), uracil (**14**–**16**), 6-azauracil (**17**) and cyanuric acid (**21**) derivatives of L-ascorbic acid with the free amino group at the *C*-4 of the lactone moiety did not show Cotton effect which is supported by a generally adopted view that the nucleophilic attack takes place with equal probability from both sides of the *C*4–*C*5 double bond resulting in racemic mixtures of enantiomers (CD spectra not shown).

2.3. Molecular and crystal structure of 6-azauracil derivative of L-ascorbic acid (**13**)

In order to establish the exact stereostructure of **13** its single crystal X-ray structure analysis was carried out. The C6–C7–C8–O3

torsion angle is $-3.0(7)°$ (Fig. 3) indicating the Z-configuration of C7–C8 double bond.

The bond lengths match very well with the corresponding ones in 5-(trifluoromethyl)uracil [22] and 6-chloropurine [23] analogues of **13**. The oxygen atoms O5 and O6 are oriented in a synperiplanar fashion; the O5–C11–C10–O6 torsion angle is 1.0(9)°. The conformation of the benzyloxy groups is antiperiplanar, defined by the C11–O5–C12–C13 and C10–O6–C19–C20 torsion angles of $-171.5(4)$ and 174.3(4)°, respectively. Two phenyl rings have different orientation with respect to the lactone ring. While the C20–C25 ring is nearly parallel with the lactone ring [dihedral angle is 7.6(2)°], the C13–C18 ring is almost perpendicular to it [dihedral angle is 73.5(2)°]. Such perpendicular orientation with respect to the lactone ring is also observed for 6-azauracil ring, as dihedral angle between their mean planes is 88.6(2)°. Three intramolecular hydrogen bonds lock the conformation of the molecule (Fig. 3; Table 2). The C6···O3 and C6···O1 hydrogen bonds form five-membered rings, while the third intramolecular hydrogen bond, C12···O6, forms six-membered ring.

The N3···O1 hydrogen bond self-assemble the molecules of **13** into dimers (Fig. 4; Table 2), so forming characteristic synthon for structures of pyrimidine derivatives, eight-membered ring.

The same hydrogen-bonding motif, centrosymmetric dimer, forms C6···O3 hydrogen bond, but this time *via* ten-membered ring. The C16···O4 hydrogen bond generates infinite chains and links hydrogen-bonded dimers (Fig. 4). Two C–H···π interactions participate also in supramolecular aggregation, so forming three-dimensional framework (Fig. 5).

2.4. Biological results

2.4.1. Cytostatic activity

Pyrimidine (**1**–**9**, **13**–**17**) and cyanuric acid derivatives of L-ascorbic acid (**19**–**22**) were evaluated *in vitro* for their cytostatic effects against malignant tumour cell lines including cervical carcinoma (HeLa), colorectal adenocarcinoma (SW620), pancreatic carcinoma (MiaPaCa-2), metastatic breast epithelial adeno
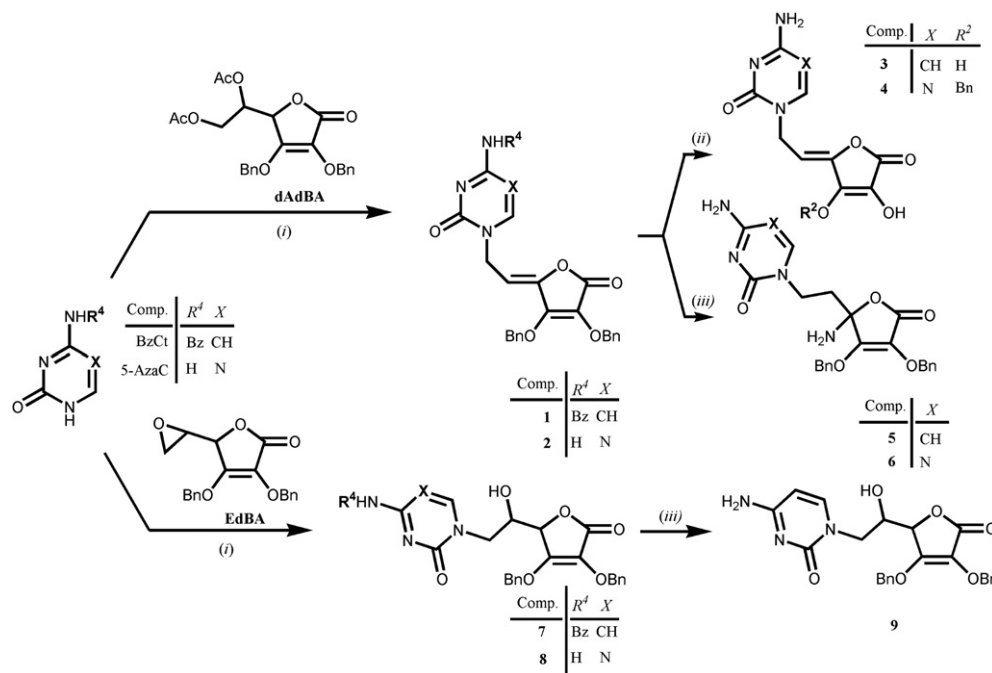
Scheme 1. Synthesis of cytosine and 5-azacytosine derivatives of L-ascorbic acid (**1**–**9**). Reagents and conditions: (*i*) HMDS, (NH$_4$)$_2$SO$_4$/argon/reflux/3 h; TMSOTf/CH$_3$CN/55–70 °C/12 h; (*ii*) BCl$_3$/CH$_2$Cl$_2$/–78 °C/2 h; (*iii*) NH$_3$/MeOH-dioxane/r.t./16 h.
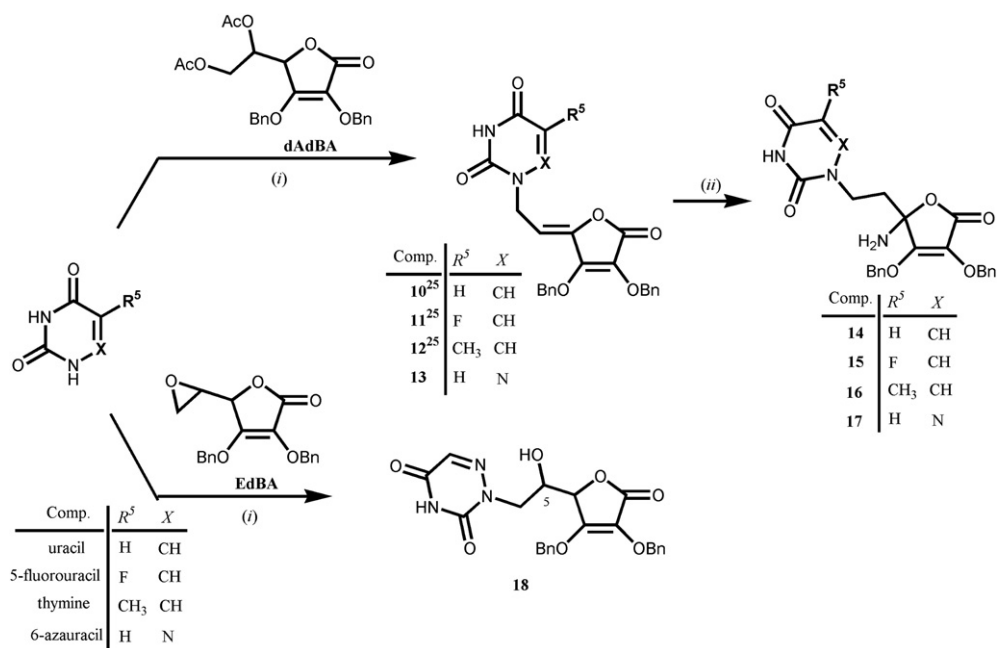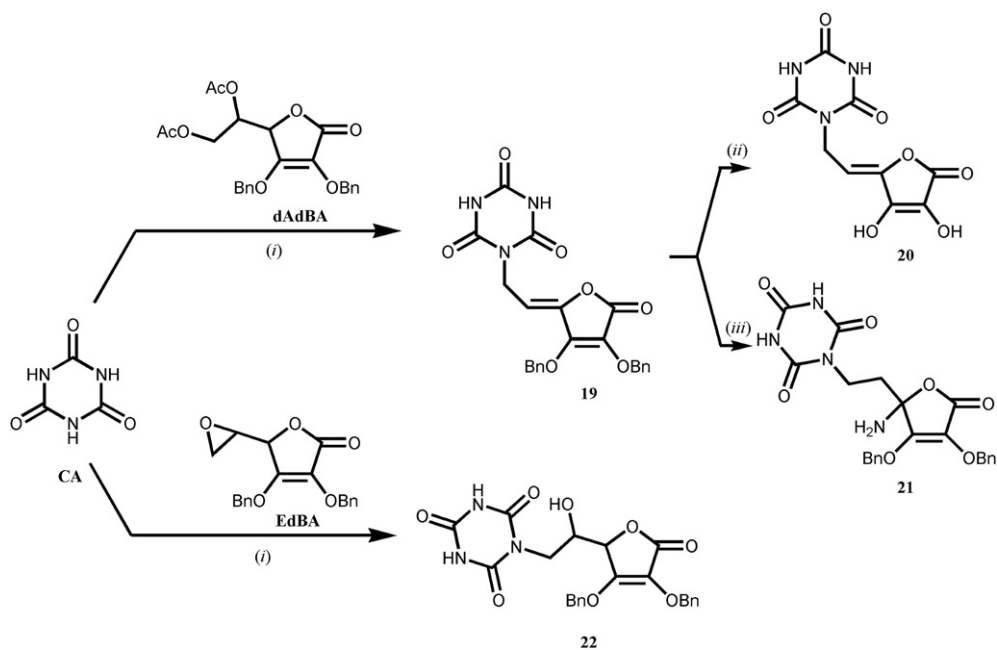
Scheme 2. Synthesis of pyrimidine derivatives of L-ascorbic acid (**10**–**18**). Reagents and conditions: (*i*) HMDS, $(NH_4)_2SO_4$/argon/reflux/3 h; TMSOTf/CH$_3$CN/55–70 °C/12 h; (*ii*) NH$_3$/MeOH-dioxane/r.t./16 h.

carcinoma (MCF-7) and hepatocellular carcinoma (HepG2), and compared with their effects on normal diploid human fibroblasts (WI38) (Table 3).

Although tested compounds did not have, in general, distinct and specific antiproliferative activity, some of them produced rather marked effects on HepG2, MCF-7, MiaPaCa-2 and HeLa cells (Fig. 6). Among these, 5-azacytosine derivative of L-ascorbic acid (**2**) with a double bond at the $C4$–$C5$ conjugated with the lactone moiety showed the most pronounced cytostatic activity, in particular towards MiaPaCa-2, HepG2 and MCF-7 cells (IC$_{50}$ 0.92, 2.72

and 3.49 μM, respectively). However, this compound was highly cytotoxic to normal human fibroblasts as well. Marked cytostatic effects were also observed in HepG2, MCF-7 and HeLa cell lines when treated with cytosine derivative of L-ascorbic acid (**1**) containing the $C4$-$C5$ double bond conjugated with the lactone moiety, with the IC$_{50}$ values of 1.98, 2.03 and 7.20, respectively. This compound also inhibited the growth of human fibroblasts. Finally, cytosine derivatives containing either enolic hydroxy groups of the lactone moiety (**3**) or free C-5 hydroxy group at the ethylenic spacer (**7** and **9**) showed stronger antiproliferative activity towards the


Scheme 3. Synthesis of cyanuric acid derivatives of L-ascorbic acid (**19**–**22**). Reagents and conditions: (*i*) HMDS, $(NH_4)_2SO_4$/argon/reflux/3 h; TMSOTf/CH$_3$CN/55-70 °C/12 h; (*ii*) BCl$_3$/CH$_2$Cl$_2$/-78 °C/2 h; (*iii*) NH$_3$/MeOH-dioxane/r.t./16 h.

Table 1
^{1}H NMR chemical shifts (δ/ppm) and H–H coupling constants (J/Hz) of compounds **1**–**9** and **13**–**22** (for enumeration of atoms in molecular skeleton *c.f.* Fig. 1A).

Comp.	H5	H6	OCH$_2$-2	OCH$_2$-3	H-4	H5′	H6′	Ph	NH$_2$-4′	NH	NH$_2$-4	OH-5
1	5.55 (t, 1H) $J=6.84$	4.67 (d, 2H) $J=6.72$	5.15 (s, 2H)	5.32 (s, 2H)	–	7.33 (d, 1H) $J=6.60$	8.16 (d, 1H) $J=6.30$	7.35–7.45 (m, 10H) 7.50–8.01 Ph$_{cyt}$ (m, 5H)	–	11.20 (s, 1H)	–	–
2	5.50 (t, 1H) $J=6.70$	4.49 (d, 2H) $J=6.74$	5.14 (s, 2H)	5.31 (s, 2H)	–	–	7.39 (s, 1H)	7.29–7.44 (m, 10H)	7,33/8,26 (s, 2 × 1H)	–	–	–
3	5.40 (t, 1H) $J=6.95$	4.59 (d, 2H) $J=6.96$	–	–	–	6.08 (d, 1H) $J=7.62$	7.99 (d, 1H) $J=7.62$)	–	8.50/9.44 (s, 2 × 1H)	–	–	–
4	5.34 (t, 1H) $J=6.87$	4.46 (d, 2H) $J=6.84$	–	5.44 (s, 2H)	–	–	7.38 (s, 1H)	7.35–7.44 (m, 10H)	7.48/8.08 (s, 2 × 1H)	–	–	–
5	1.85–2.03 (m,2H)	3.60 (t, 2H) $J=7.35$	5.01 (s, 2H)	5.13 (dd, 2H) $J_1=11,83$ $J_2=22,93$	–	5.61 (d, 1H) $J=7,14$	7.37 (d,1H) $J=7,15$	7.32–7.40 (m, 10H)	6.93/6.99 (s, 2 × 1H)	–	6,11/8,17 (s, 2x1H)	–
6	1.92–2.06 (m, 2H)	3.62–3.72 (m, 2H)	5.01 (s, 2H)	5.13 (dd, 2H) $J_1=11.83$ $J_2=41.37$	–	–	7.31 (s, 1H)	7.30–7.41 (m, 10H)	7.35/8.17 (s, 2 × 1H)	–	6.12/8.09 (s, 2x1H)	–
7	4.11–4.16 (m, 1H)	3.70/4.23 (2 × dd, 2H) $J_1=9.78/2.46$ $J_2=13.08/13.08$	4.96 (dd, 2H) $J_1=11,13$ $J_2=17,49$	5.23 (dd, 2H) $J_1=11.64$ $J_2=51.13$	4.99 (s, 1H)	5.58 (d, 1H) $J=6.90$	8.07 (d, 1H) $J=7.20$)	7.29–7.41 (m, 10H) 7.49–8.00 Ph$_{cyt}$ (m, 5H)	–	11.16 (s, 1H)	–	5.42 (d, 1H) $J=6.77$
8	3.98–4.08 (m, 1H)	3.49–4.08 (m, 2H)	4.95 (s, 2H)	5.20 (dd, 2H) $J_1=11.69$ $J_2=26.58$	4.98 (s, 1H)	–	7.35 (s, 1H)	7.26–7.40 (m, 10H)	7.38/8.12 (s, 2 × 1H)	–	–	5.47 (d, 1H) $J=6.75$
9	4.00–4.07 (m, 1H)	3.45–4.07 (m, 2H)	4.90 (s, 2H)	5.22 (dd, 2H) $J_1=11.71$ $J_2=24.73$	4.96 (d, 2H) $J=1.68$	5.62 (d, 1H) $J=7.14$	7.48 (d, 1H) $J=7.16$	7.28–7.38 (m, 10H)	6.95/7.02 (s, 2 × 1H)	–	–	5.54 (d, 1H) $J=6.84$
13	5.51 (t, 1H) $J=6.74$	4.69 (d, 2H) $J=6.71$	5.16 (s, 2H)	5.33 (s, 2H)	–	7.47 (s, 1H)	–	7.35–7.45 (m, 10H)	–	12.16 (s, 1H)	–	–
14	1.96 (m, 2H)	3.64 (dd, 2H) $J_1=6.20$ $J_2=13.71$	5.01 (s, 2H)	5.14 (dd, 2H) $J_1=11.91$ $J_2=22.41$	–	7.45 (d, 1H) $J=7.86$)	5.51 (dd, 1H) $J_1=1.68$ $J_2=7.77$	7.33–7.42 (m, 10H)	–	11.21 (s, 1H)	6.16/8.17 (s, 2 × 1H)	–
15	1.93–2.08 (m, 2H)	3.58–3.72 (m, 2H)	5.01 (s, 2H)	5.14 (dd, 2H) $J_1=11.87$ $J_2=39.36$	–	–	7.91 (d, 1H) $J=3.39$	7.31–7.41 (m, 10H)	–	11.73 (s, 1H)	6.17/8.16 (s, 2 × 1H)	–
16	1.86–2.03 (m, 2H)	3.52–3.66 (m, 2H)	4.99 (s, 2H)	5.11 (dd, 2H) $J_1=11.89$ $J_2=24.01$	–	–	7.33 (s, 1H)	7.27–7.40 (m, 10H)	–	11.19 (s, 1H)	6.13/8.13 (s, 2 × 1H)	–
17	1.94–2.08 (m, 2H)	3.82–3.92 (m, 2H)	5.03 (s, 2H)	5.15 (dd, 2H) $J_1=11.94$ $J_2=41.12$	–	7.46 (s, 1H)	–	7.20–7.44 (m, 10H)	–	1208 (s, 1H)	6.14/8.12 (s, 2 × 1H)	–
18	3.93–4.04 (m, 1H)	3.93–4.04 (m, 1H)	4.97 (s, 2H)	5.20 (dd, 2H) $J_1=11,79$ $J_2=35, 05$	4.96 (s, 1H)	7.44 (s, 1H)	–	7.29–7.41 (m, 10H)	–	12, 05 (s, 1H)	–	5.49 (d, 1H) $J=6.16$
19	5.42 (t, 1H) $J=6.18$	4.48 (d, 2H) $J=6.10$	5.14 (s, 2H)	5.31 (s, 2H)	–	–	–	7.30–7.45 (m, 10H)	–	11.43 (s, 2H)	–	–
20	5.31 (t, 1H) $J=6.37$	4.47 (d, 2H) $J=6.31$	–	–	–	–	–	–	–	11.47 (s, 2H)	–	–
21	1.83–2.01 (m, 2H)	3.58–3.76 (m, 2H)	5.00 (s, 2H)	5.11 (dd 2H) $J_1=11.85$ $J_2=37.33$	–	–	–	7.34–7.39 (m, 10H)	–	11.34 (s, 2H)	6.08/8.17 (s, 2 × 1H)	–
22	3.96–4.05 (m, 1H)	3.46–4.05 (m, 2H)	4.94 (s, 2H)	5.20 (dd, 2H) $J_1=11.67$ $J_2=26.54$	4.98 (s, 1H)	–	–	7.27–7.42 (m, 10H)	–	11.45 (s, 2H)	–	–

Compounds were dissolved in DMSO-d_6. **3**: 9.67 ppm (OH-3, s, 1H), 11.32 ppm (OH-2, s, 1H); **4**: 9.75 ppm (OH-2; s, 1H); **16**: 1.72 ppm (CH$_3$, s, 3H); **20**: 9.53 ppm (OH-3, s, 1H), 11.24 ppm (OH-2, s, 1H).
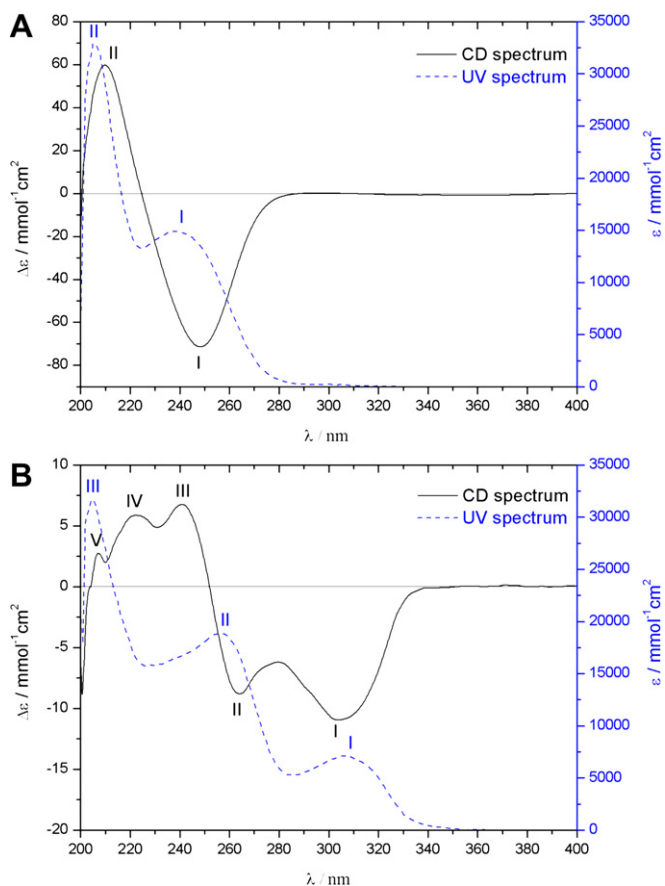
Fig. 2. A. CD (—, $c = 3000 \times 10^{-5}$ mol dm^{-3}, $l = 1$ cm) and UV (−−, $c = 2442 \times 10^{-3}$ mol dm^{-3}, $l = 1$ cm) spectra of **8** in EtOH. B. CD (—, $c = 2993 \times 10^{-5}$ mol dm^{-3}, $l = 1$ cm) and UV (−−, $c = 2993 \times 10^{-5}$ mol dm^{-3}, $l = 1$ cm) spectra of **7** in EtOH.

MCF-7 cells in comparison with other tested tumour cell lines, but it also exerted rather marked cytotoxic effect on normal fibroblasts.

2.4.2. Cell cycle progression

As compounds **1** and **2** exerted the most pronounced cytostatic activities in tested cell lines, we monitored their effects on the cell cycle (Tables 4 and 5). Compound **2** had specific impact on the progression of MiaPaCa-2, SW620 and HeLa cell cycle causing significant decline in G1 phase cells accompanied by marked accumulation of cells in S phase (Table 5). This cell cycle pattern was uniformly observed across all three tested cell lines, except for MiaPaCa-2 cells treated with lower concentration of compound **2** for 24 h. Based on obtained data, it seems reasonable to believe that observed cell growth inhibition upon treatment with compound **2** is attributable to its interference with cell replication. Observed effect indeed, might be partially attributed to the 5-azacytidine's general toxicity reported previously [30]. 5-azacytidine could be activated to the nucleoside triphosphate and incorporated into both DNA and RNA resulting in the inhibition of DNA, RNA and protein synthesis [31]. When applied at doses low enough to avoid induction of cell death, incorporation of 5-azacytidine into DNA of cultured cells promotes a rapid loss of activity of DNA (cytosine-C5) methyltransferase, as this enzyme binds irreversibly to ZCyt residues in DNA [32]. If not repaired, this complex is toxic and mutagenic in bacteria, cultured cells and rodents [33]. It still remains to be elucidated whether 5-azacytidine inhibits growth primarily through cytotoxicity or through the effects on DNA methylation. Anticancer potential of compound **2** is corroborated by its ability to

interfere with DNA replication mechanisms in cancer cells at low pharmacological concentrations (1 μM and 5 μM) even if these micromolar concentrations failed to induce apoptosis in all cell lines (data not shown). Knowing that drug potency (IC$_{50}$ values obtained in the *in vitro* studies) was found to be predictive of Phase II performance/toxicity of the tested drugs [34,35], additional *in vivo* studies should be preformed to investigate the possible use of compound **2** as a novel anticancer pro-drug. On contrary, compound **1** showed neither specific nor significant effect on HeLa and MCF-7 cell cycle (Table 4) and apoptosis induction at micromolar concentrations (5 μM and 10 μM), except for inducing a rise in S- phase HeLa cells after 24-h treatment at 10 μM. This finding raises a question whether higher pharmacological concentrations of this substance would induce non-specific cytotoxic effects, and might not be suitable to achieve desired biological effect *in vivo*.

3. Experimental section

3.1. Materials and general methods

Melting points were determined on a Kofler micro hot-stage instrument (Reichter, Wien) and were uncorrected. ^{1}H and ^{13}C NMR spectra were recorded on a Varian Gemini 300 spectrometer, operating at 300 and 75.5 MHz for the ^{1}H and ^{13}C nuclei, respectively. Samples were measured in DMSO-d_6 solutions at 20 °C in 5 mm NMR tubes. Chemical shifts (δ) in ppm were referred to TMS. The electron impact mass spectra were recorded with an EXTERNAL FT MS 2002 instrument with ionizing energy of 70 eV. Precoated Merck silica gel 60 F$_{254}$ plates were used for thin-layer chromatography. Spots were visualized by shortwave (254 nm) UV light. Column chromatography was performed on Fluka silica gel (0.063−0.200 mm), with dichloromethane/methanol and petrolether/ethylacetate as eluent. Additional purification of some compounds by recrystallization from ethanol afforded the analytical samples.

All chemicals were purchased from Sigma Aldrich (Germany). All solvents were of analytical grade purity and dried. Dichloromethane (CH$_2$Cl$_2$) was distilled from phosphorus pentoxide (P$_2$O$_5$) and stored over 4Å molecular sieves. Acetonitrile (CH$_3$CN) was distilled from calcium hydride (CaH$_2$) and stored over 3 Å molecular sieves. Methanol (CH$_3$OH) was not distilled but stored over 3 Å molecular sieves.

3.2. Synthesis

3.2.1. Method A. General procedure for the preparation of pyrimidine derivatives of 2,3-di-O-benzyl-4,5-didehydro-5,6-dideoxy-L-ascorbic acid (1, 2, 13 and 19)

Suspension of anhydrous base (1.5 g) and (NH$_4$)$_2$SO$_4$ (110 mg) in HMDS (30 mL) was refluxed overnight under the inert atmosphere of argon. The excess HMDS was removed under the reduced pressure (0.1 mmHg). To the oily product thus obtained 5,6-di-O-acetyl-2,3-di-O-benzyl-L-ascorbic acid (n$_{base}$/1.507 mmol) dissolved in dry CH$_3$CN (15 mL) was added. Then TMSOTf (4 × 0.2 mL) was added dropwise at room temperature and the mixture stirred for 16 h at 55−70 °C. The reaction mixture was evaporated and the crude oily product washed with CH$_2$Cl$_2$ and several times with aq. NaHCO$_3$. Organic layer was dried over MgSO$_4$, evaporated, and the crude product purified by silica gel column chromatography.

3.2.2. Method B. General procedure for the preparation of pyrimidine derivatives with the amino group at the C-4 of L-ascorbic acid (5, 6, 14–17 and 21)

To a solution of pyrimidine derivatives of L-ascorbic acid (0.13 mmol) in dioxane (10 mL) and methanol (10 mL) ammonia (g)
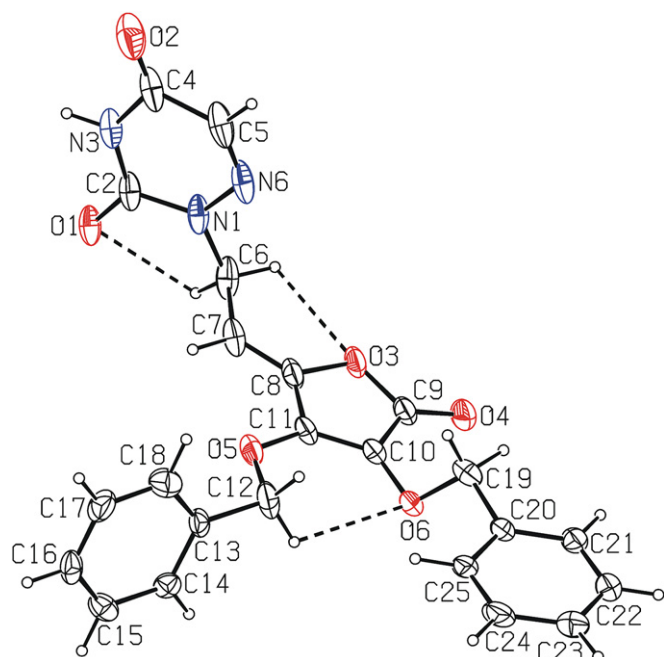
Fig. 3. A view of **13**, with the atom-numbering scheme. Displacement ellipsoids for non-hydrogen atoms are drawn at the 20% probability level. Intramolecular hydrogen bonds are indicated by dashed lines.

was introduced at 0 °C. The reaction mixture was stirred at room temperature for 24 h, then concentrated under reduced pressure and the crude product purified by silica gel column chromatography.
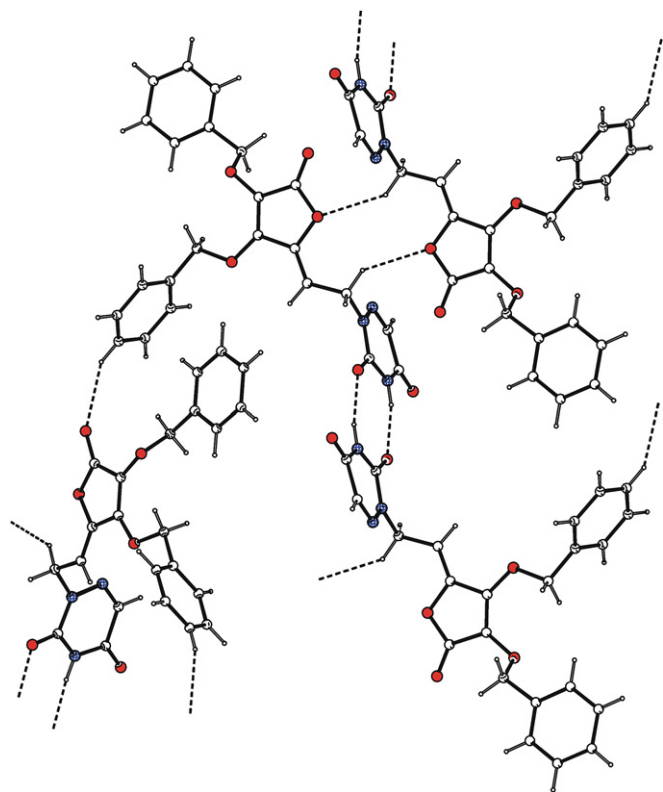
Table 2
Hydrogen-bonding and C−H···π interactions geometry for **13**.

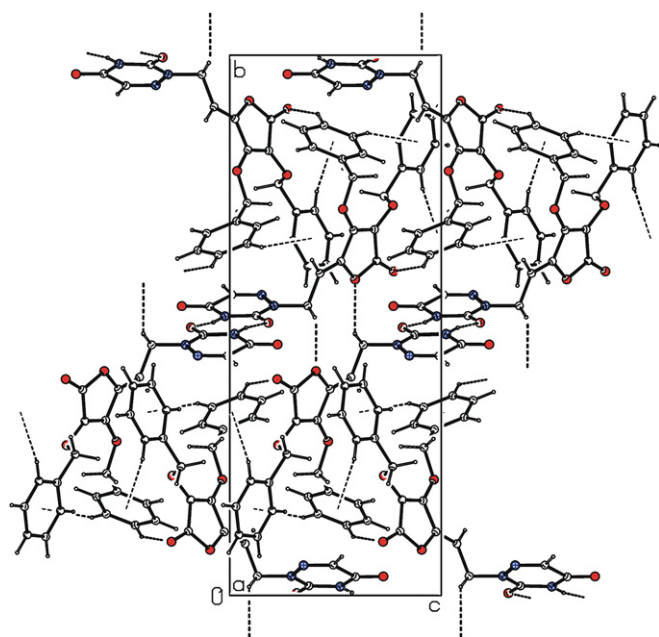| D−H···A	D−H (Å)	H···A (Å)	D···A (Å)	D−H···A (°)	Symmetry codes
C6−H6A···O3	0.99	2.50	2.912(6)	105	
C6−H6B···O1	0.99	2.37	2.777(5)	104	
C12−H12B···O6	0.99	2.50	2.989(6)	110	
N3−H3···O1	0.89(6)	1.97(6)	2.849(5)	168(4)	$1 - x, 1 - y, -z$
C6−H6A···O3	0.99	2.60	3.422(5)	141	$2 - x, 1 - y, 1 - z$
C16−H16···O4	0.95	2.49	3.359(5)	152	$-1 + x, 3/2 - y, -1/2 + z$
C15−H15···Cg1[a]	0.95	2.60	3.489(5)	157	$-1 + x, y, z$
C21−H21···Cg2[a]	0.95	2.78	3.708(5)	168	$1 + x, 3/2 - y, 1/2 + z$

[a] Cg1 and Cg2 are the centroids of C20−C25 and C13−C18 rings, respectively.

3.2.3. Method C. General procedure for the preparation of pyrimidine derivatives of 2,3-di-O-benzyl-6-deoxy-L-ascorbic acid (7, 8, 18 and 22)

The suspension of anhydrous pyrimidine base (1.5 g) and $(NH_4)_2SO_4$ (100 mg) in HMDS (30 mL) was refluxed for 3 h in the inert atmosphere of argon. Excess HMDS was evaporated under the reduced pressure. To the oily product thus obtained, 4-(5,6-epoxy)-2,3-di-O-benzyl-L-ascorbic acid (0.30 mmol) in CH_3CN (5 mL) was added. Then, TMSOTf was added in portions (0.5 mL; 2.76 mmol) and the reaction mixture heated for 12 h at 55−70 °C. The solvent was evaporated and the residue portioned between CH_2Cl_2 and saturated aq. NaHCO$_3$. Organic layer was dried over MgSO$_4$, evaporated and the residue submitted to silica gel column chromatography.

3.2.4. Method D. General procedure for the preparation of debenzylated pyrimidine derivatives of 4,5-didehydro-5,6-dideoxy-L-ascorbic acid (3, 4 and 20)

To a solution of 2,3-O-dibenzylated derivatives of L-ascorbic acid (**1**, **2** and **19**) (0.42 mmol) in anhydrous CH_2Cl_2 (7 mL) 1M solution of BCl_3 in CH_2Cl_2 (0.5 mL) was added under argon at −78 °C. The reaction mixture was stirred at −40 °C for 4 h, and additional amount of 1M BCl_3 in CH_2Cl_2 (0.5 mL) was added. The reaction mixture was then stirred at 0 °C for 2 h. Thereafter, the temperature was raised to room temperature and the reaction mixture stirred

Fig. 4. A part of the crystal structure of **13**, showing N−H···O and C−H···O hydrogen bonds. Hydrogen bonds are indicated by dashed lines.

Fig. 5. A crystal packing diagram of **13**, viewed along the *a* axis, showing three-dimensional framework formed by one N−H···O and two C−H···O hydrogen bonds, as well as two C−H···π interactions. Hydrogen bonds and C−H···π interactions are indicated by dashed lines.

Table 3
Inhibitory effects of pyrimidine (**1–9, 13–17**) and cyanuric acid derivatives of L-ascorbic acid (**19–22**) on the growth of malignant tumor cell lines in comparison with their effects on the growth of normal diploid human fibroblasts (WI38).
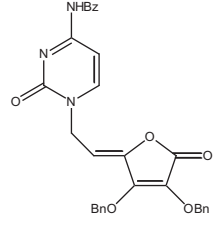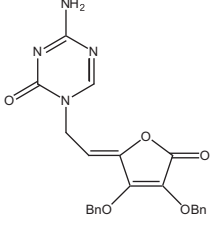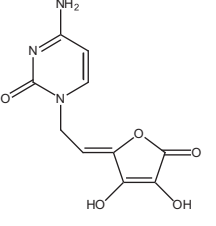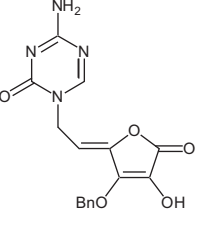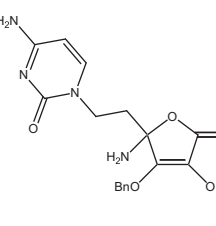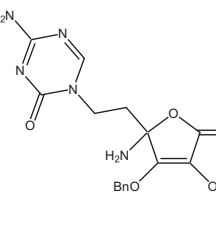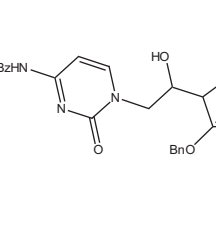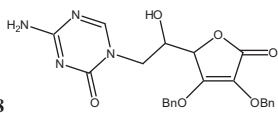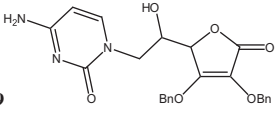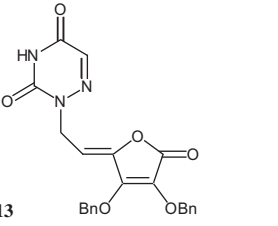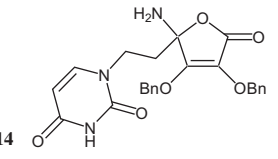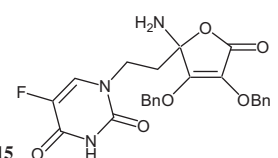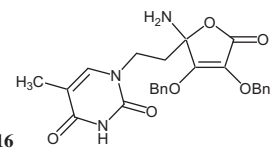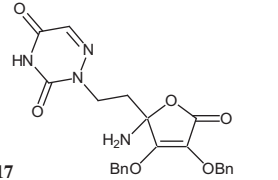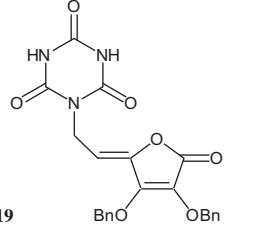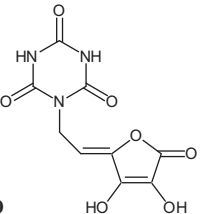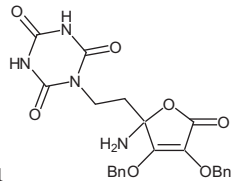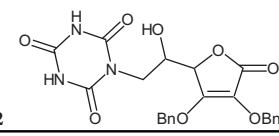
Compd.	Tumor cell growth IC$_{50}$[a] (µM)					
	HeLa	MCF-7	HepG2	SW620	MiaPaCa-2	WI38
1	7.20	2.03	1.98	>100	24.24	8.49
2	5.91	3.49	2.72	5.62	0.92	4.67
3	>100	8.92	23.50	>100	>100	54.27
4	>100	>100	>100	>100	>100	>100
5	>100	31.99	>100	>100	>100	88.89
6	>100	>100	>100	>100	>100	>100
7	35.88	4.79	62.19	>100	>100	8.82

Table 3 (continued)

Compd.	Tumor cell growth IC$_{50}$^{a} (µM)					
	HeLa	MCF-7	HepG2	SW620	MiaPaCa-2	WI38
8	>100	73.76	>100	>100	71.68	>100
9	>100	7.34	44.31	>100	>100	53.94
13	44.96	3.77	41.28	36.51	20.37	24.62
14	>100	>100	>100	>100	>100	>100
15	>100	20.87	42.80	>100	>100	36.24
16	>100	80.35	>100	>100	>100	>100
17	>100	>100	>100	>100	>100	>100
19	>100	17.84	44.75	>100	37.94	0.01

Table 3 (continued)

Compd.	Tumor cell growth IC$_{50}$[a] (μM)					
	HeLa	MCF-7	HepG2	SW620	MiaPaCa-2	WI38
20	>100	>100	>100	>100	>100	35.26
21	77.12	84.91	>100	>100	>100	>100
22	>100	>100	>100	>100	>100	>100

[a] IC$_{50}$; 50% inhibitory concentration, or compound concentration required to inhibit tumor cell proliferation by 50%.

overnight. A solvent mixture of CH$_2$Cl$_2$/CH$_3$OH (1:1) was added to deactivate the unreacted BCl$_3$ and the solvent was subsequently removed under reduced pressure. The oily residue was purified by silica gel column chromatography.

3.2.5. N-{1-[2-(3,4-bis-benzyloxy-5-oxo-5H-furan-2-ylidene)-ethyl]-2-oxo-1,2-dihydro-pyrimidin-4-yl}-benzamide (1)

Using a procedure described in method A a mixture of N^4-benzoylcytosine (1.5 g; 6.97 mmol) and **dAdBA** (2.01 g; 4.57 mmol) gave the crude product that was purified by silica gel column cromatography (CH$_2$Cl$_2$/CH$_3$OH = 90:1). Recrystallization from ethanol afforded Z-isomer of **1** as white crystals (349 mg; 13.89%; m.p. 175−177 °C).

^{13}C NMR (DMSO-d_6): δ 45.37 (C-6), 73.53 (O$\underline{C}$H$_2$-2), 74.57 (O$\underline{C}$H$_2$-3), 96.68 (C-5′), 104.02 (C-5), 123.43 (C-2), 128.43−133.33 ($\underline{C}_6$H$_5$), 135.87 (C-2a), 135.90 (C-3a), 143.10 (C-3), 148.58 (C-4), 150.71 (C-6′), 163.76 (C-1), 164.23 (C-4′), 165.45 (C-2′), 166.12 (C-4′). MS m/z 536.5 [M + 1].

3.2.6. 4-Amino-1-[2-(3,4-bis-benzyloxy-5-oxo-5H-furan-2-ylidene)-ethyl]-1H-[1,3,5]triazin-2-one (2)

Reaction of silylated 5-azacytosine (1.5 g; 13.4 mmol) and **dAdbA** (2 g; 4.54 mmol) according to method A gave a crude product which was submitted to silica gel column chromatography (CH$_2$Cl$_2$/CH$_3$OH = 60:1) and subsequent recrystallization from ethanol to afford compound **2** (Z-isomer) as white crystals (60 mg; 3.06%; m.p. 177−178 °C).

^{13}C NMR (DMSO-d_6): δ 42.40 (C-6), 73.44 (O$\underline{C}$H$_2$-2), 74.49 (O$\underline{C}$H$_2$-3), 104.52 (C-5), 123.35 (C-2), 128.38−135.89 ($\underline{C}_6$H$_5$), 135.89 (C-2a), 136.24 (C-3a), 142.61 (C-3), 148.61 (C-4), 154.10 (C-4′), 159.54 (C-6′), 164.20 (C-1), 166.92 (C-2′). MS m/z 433.1; 434.1 [M + 1; M + 2].

3.2.7. 4-Amino-1-[2-(3,4-dihydroxy-5-oxo-5H-furan-2-ylidene)-ethyl]-1H-pyrimidin-2-one (3)

To a solution of **1** (250 mg; 0.47 mmol) in dry CH$_2$Cl$_2$ in accordance with method D the crude product obtained was purified by column chromatography (CH$_2$Cl$_2$/CH$_3$OH = 5:1) yielded **3** as white crystals (20 mg; 17.05%; m.p. > 300 °C).

^{13}C NMR (DMSO-d_6): δ 44.39 (C-6), 94.01 (C-5′), 99.50 (C-5), 122.03 (C-2), 143.09 (C-3), 145.36 (C-4), 147.97 (C-2′), 150.02 (C-6′), 160.12 (C-4′), 164.94 (C-1). MS m/z 252.2 [M + 1].

3.2.8. 4-Amino-1-[2-(3-benzyloxy-4-hydroxy-5-oxo-5H-furan-2-ylidene)-ethyl]-1H-[1,3,5]triazin-2-one (4)

To a solution of **2** (197 mg; 0.46 mmol) in dry dichloromethane according to method D the crude product was obtained and separated by silica gel column chromatography (CH$_2$Cl$_2$/CH$_3$OH = 10:1) to afford **4** as colorless oil (25 mg; 15.88%).

^{13}C NMR (DMSO-d_6): δ 41.74 (C-6), 72.18 (O$\underline{C}$H$_2$-3), 101.18 (C-5), 123.24 (C-2), 127.90−128.54 ($\underline{C}_6$H$_5$), 136.14 (C-3a), 141.22 (C-3), 143.45 (C-4), 153.61 (C-4′), 158.99 (C-6′), 164.61 (C-1), 166.40 (C-2′). MS m/z 343.2 [M + 1].

3.2.9. 4-Amino-1-[2-(2-amino-3,4-bis-benzyloxy-5-oxo-2,5-dihydro-furan-2-yl)-ethyl]-1H-pyrimidin-2-one (5)

Compound **1** was treated with saturated methanolic ammonia in accordance with method B. The reaction mixture was then concentrated under reduced pressure and the residue was purified by silica gel column chromatography (CH$_2$Cl$_2$/CH$_3$OH = 5:1) to give **5** as white crystals (110 mg; 43.79%; m.p. 168−170 °C).

^{13}C NMR (DMSO-d_6): δ 36.47 (C-5), 45.08 (C-6), 72.52 (O$\underline{C}$H$_2$-2), 73.53 (O$\underline{C}$H$_2$-3), 82.33 (C-4), 93.75 (C-5′), 123.53 (C-2), 128.19−129.23 ($\underline{C}_6$H$_5$), 136.90 (C-2a), 137.29 (C-3a), 146.38 (C-6′), 154.02 (C-3), 156.18 (C-2′), 166.38 (C-4′), 168.40 (C-1). MS m/z 449.3 [M + 1].

3.2.10. 4-Amino-1-[2-(2-amino-3,4-bis-benzyloxy-5-oxo-2,5-dihydro-furan-2-yl)-ethyl]-1H-[1,3,5]triazin-2-one (6)

Solution of **3** (149 mg; 0.28 mmol) was treated as described in method B. The residue was purified by silica gel column chromatography (CH$_2$Cl$_2$/CH$_3$OH = 5:1). The pale-yellow crystals obtained were additionally recrystallized from ethanol and washed with distilled water to yield **6** as white crystals (52 mg; 18.71%, m.p. 194−196 °C).

^{13}C NMR (DMSO-d_6): δ 35.39 (C-5), 42.59 (C-6), 72.08 (O$\underline{C}$H$_2$-2), 73.27 (O$\underline{C}$H$_2$-3), 81.97 (C-4), 123.14 (C-2), 127.66−128.49 ($\underline{C}_6$H$_5$), 136.34 (C-2a), 136.78 (C-3a), 153.46 (C-3), 153.82 (C-2′), 159.11 (C-6′), 166.39 (C-4′), 167.86 (C-1). MS m/z 450.1; 451.1 [M + 1; M + 2].

3.2.11. N-{1-[2-(3,4-bis-benzyloxy-5-oxo-2,5-dihydro-furan-2-yl)-2-hydroxy-ethyl]-2-oxo-1,2-dihydro-pyrimidin-4-yl}-benzamide (7)

A mixture of N^4-benzoylcytosine (220 mg; 1.01 mmol) and 4-(5,6-epoxy)-2,3-O,O-dibenzyl-L-ascorbic acid (100 mg; 0.30 mmol)
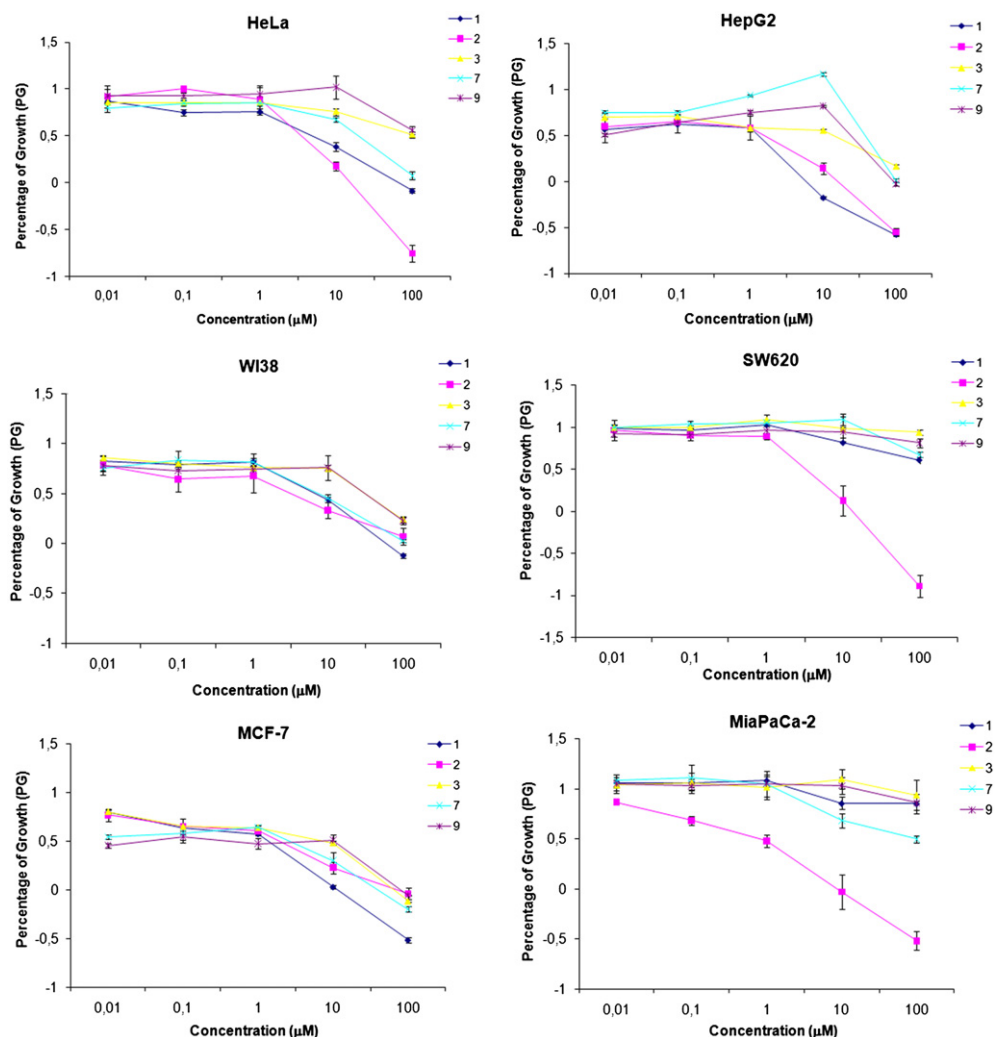
Fig. 6. Concentration-response curves for compounds **1, 2, 3, 7** and **9** on tested tumour cell lines (HeLa, HepG2, MCF-7, MiaPaCa-2 and SW620) and normal human fibroblasts (WI38). The percentages of growth (PG) were calculated.

according to method C gave yellow oil. The crude product was separated by silica gel column chromatography ($CH_2Cl_2/CH_3OH = 50:1$) to afford **7** as white crystals (53 mg; 32.40%; m.p. 89–91 °C).

^{13}C NMR (DMSO-d_6): δ 53.29 (C-6), 64.82 (C-5), 72.79 (O$\underline{C}H_2$-2), 73.62 (O$\underline{C}H_2$-3), 75.88 (C-4), 95.43 (C-5′), 120.79 (C-2), 127.83−133.13 ($\underline{C}_6H_5$), 135.56 (C-2a), 136.12 (C-3a), 151.55 (C-6′), 155.36 (C-3), 157.41 (C-2′), 163.19 (C-4′), 167.16 (C-1), 169.08 (C-4″). MS m/z 554.5 [M + 1].

*3.2.12. 4-Amino-1-[2-(3,4-bis-benzyloxy-5-oxo-2,5-dihydro-furan-2-yl)-2-hydroxy-ethyl]-1H-pyrimidin-2-one (**8**)*

The removal of the benzoyl protecting group of the compound **7** (220 mg; 0.4 mmol) was achieved using methanolic ammonia (method C). The residue was submitted to silica gel column chromatography ($CH_2Cl_2/CH_3OH = 10:1$) to afford **8** as white crystals (130 mg; 72.30%; m.p. 118−120 °C).

Table 4
Effect of compound **1** on the cell cycle progression. The results are presented as percentage of particular cell population (%) ± standard deviation. Significant results ($p > 0.05$) are denoted in bold and marked with *.

Cell line	Treatment Duration (h)	Treatment regimen	Cell cycle phase (%)			
			G1	G2/M	S	SubG1
HeLa	24	no treatment	44.8 ± 11.2	10.9 ± 2.6	44.4 ± 8.7	0.49 ± 0.2
		5 μM	47.1 ± 0.1	13.1 ± 0.1	39.9 ± 0.1	0.04 ± 0.01
		10 μM	37.9 ± 1.8	8.45 ± 6.3	**53.7 ± 4.5***	0.20 ± 0.01
	48	No treatment	56.1 ± 0.1	3.25 ± 0.1	40.6 ± 0.1	0.16 ± 0.01
		5 μM	60.8 ± 0.1	2.8 ± 0.1	36.5 ± 0.1	0.27 ± 0.01
		10 μM	52.3 ± 0.1	8.3 ± 0.1	39.5 ± 0.1	0.56 ± 0.01
MCF-7	24	No treatment	50.7 ± 3.1	15.9 ± 2.7	33.4 ± 0.4	0.68 ± 0.4
		5 μM	57.9 ± 0.1	13.8 ± 0.1	28.3 ± 0.1	0.42 ± 0.01
		10 μM	54.3 ± 5.9	6.54 ± 5.1	39.2 ± 1	0.20 ± 0.1
	48	No treatment	52.3 ± 6.1	6.82 ± 0.3	40.9 ± 5.7	0.51 ± 0.01
		5 μM	50. 6 ± 7	13.9 ± 6.4	35.6 ± 0.6	0.37 ± 0.2
		10 μM	56.6 ± 0.9	5.52 ± 0.7	38 ± 1.5	0.32 ± 0.3

Table 5
Effect of compound **2** on the cell cycle progression. The results are presented as percentage of particular cell population (%) ± standard deviation. Significant results ($p > 0.05$) are denoted in bold and marked with *.

Cell line	Treatment Duration (h)	Treatment regimen	Cell cycle phase (%)			
			G1	G2/M	S	SubG1
MiaPaCa-2	24	no treatment	55.4 ± 0.01	10.3 ± 0.07	34.3 ± 0.07	0.32 ± 0.009
		1 μM	55.6 ± 0.14	14.9 ± 0.07	29.5 ± 0.07	0.20 ± 0.008
		5 μM	**35.6 ± 2.76***	7.05 ± 1.34	**57.4 ± 1.41***	0.21 ± 0.05
	48	no treatment	44.7 ± 7.21	9.35 ± 0.92	46 ± 8.13	0.20 ± 0.06
		1 μM	**22.9 ± 0.07***	12.9 ± 0.01	**64.2 ± 0.01***	0.18 ± 0.009
		5 μM	**29 ± 2.05***	10.2 ± 0.85	**60.9 ± 1.2***	0.31 ± 0.15
SW620	24	no treatment	51.6 ± 0.07	10.7 ± 0.07	37.7 ± 0.01	0.37 ± 0.36
		1 μM	**41.3 ± 4.81***	8.15 ± 2.9	**50.5 ± 1.98***	0.56 ± 0.31
		5 μM	**24.1 ± 0.07***	**17.7 ± 0.07***	**58.3 ± 0.07***	0.20 ± 0.004
	48	No treatment	46.6 ± 4.88	11.9 ± 2.33	41.7 ± 2.47	0.18 ± 0.036
		1 μM	**23.2 ± 0.07***	**17.9 ± 0.07***	**58.9 ± 0.07***	0.05 ± 0.0024
		5 μM	**39.1 ± 1.06***	9.2 ± 5.94	**51.8 ± 4.88***	0.21 ± 0.05
HeLa	24	no treatment	56 5 ± 8.27	9.2 ± 4.38	34.8 ± 3.82	0.02 ± 0.008
		1 μM	**29.4 ± 5.59***	11.9 ± 6.65	**58.8 ± 1.06***	0
		5 μM	**16.5 ± 0.21***	11.5 ± 1.63	**72.1 ± 1.41***	0
	48	No treatment	64.1 ± 2.62	11.5 ± 0.57	24.5 ± 3.18	0.02 ± 0.016
		1 μM	**20.1 ± 0.07***	14.4 ± 0.01	**65.6 ± 0.01***	0.02 ± 0.005
		5 μM	**23.9 ± 0.01***	13.9 ± 0.01	**62.3 ± 0.01***	0.23 ± 0.005

^{13}C NMR (DMSO-d_6): δ 52.27 (C-6), 66.52 (C-5), 72.96 (O$\underline{C}$H$_2$-2), 73.93 (O$\underline{C}$H$_2$-3), 75.24 (C-4), 94.63 (C-5′), 120.65 (C-2), 129.47–133.64 ($\underline{C}_6$H$_5$), 135.29 (C-2a), 136.31 (C-3a), 152.83 (C-6′), 154.27 (C-3), 157.41 (C-2′), 162.59 (C-4′), 166.92 (C-1). MS m/z 450.4 [M + 1].

3.2.13. 4-Amino-1-[2-(3,4-bis-benzyloxy-5-oxo-2,5-dihydro-furan-2-yl)-2-hydroxy-ethyl]-1H-[1,3,5]triazin-2-one (9)

Reaction of 5-azacytosine (678 mg; 6.05 mmol) and epoxy derivative of L-ascorbic acid (600 mg; 1.77 mmol) as described in method C afforded yellow oil. The crude product was separated by silica gel column chromatography (CH$_2$Cl$_2$/CH$_3$OH = 20:1) to obtain **9** as white crystals (217 mg; 27.20%; m.p. 148–150 °C).

^{13}C NMR (DMSO-d_6): δ 50.47 (C-6), 65.33 (C-5), 73.29 (O$\underline{C}$H$_2$-2), 74.12 (O$\underline{C}$H$_2$-3), 76.29 (C-4), 121.29 (C-2), 128.25–129.17 ($\underline{C}_6$H$_5$), 136.09 (C-2a), 136.62 (C-3a), 154.55 (C-3), 157.90 (C-2′), 160.16 (C-6′), 167.00 (C-1), 169.54 (C-4′). MS m/z 451.1 [M + 1].

3.3. General procedure for the synthesis of pyrimidine derivatives of 4,5-didehydro-5,6-dideoxy-L-ascorbic acid

The synthesis of pyrimidine derivatives of L-ascorbic acid (**10–12**) with a double bond in the C4-C5 position was previously described [23].

3.3.1. 2-[2-(3,4-bis-benzyloxy-5-oxo-5H-furan-2-ylidene)-ethyl]-2H-[1,2,4]triazine-3,5-dione (13)

Condensation of 6-azauracil (1.5 g; 13.27 mmol) and **dAdBA** in accordance with method A gave yellow oil as a crude product which was purified by silica gel column chromatography (petrolether/EtOAc = 3:1). Compound **13** was isolated as white crystals that were recrystallized from ethanol (180 mg; 9.15%; m.p. 80–84 °C).

^{13}C NMR (DMSO-d_6): δ 45.20 (C-6), 72.99 (O$\underline{C}$H$_2$-2), 73.97 (O$\underline{C}$H$_2$-3), 103.33 (C-5), 122.89 (C-2), 127.94–128.78 ($\underline{C}_6$H$_5$), 135.38 (C-2a), 135.74 (C-3a), 135.74 (C-5′), 142.29 (C-3), 148.04 (C-4), 148.06 (C-2′), 150.71 (C-6′), 157.08 (C-4′), 163.68 (C-1). MS m/z 434.1 [M + 1].

3.4. General procedure for ammonolysis of pyrimidine derivatives 10–13

Pyrimidine derivatives (**10–13**) (0.13 mmol) were treated with methanolic ammonia as described in method B. The residue was subjected to column chromatography (CH$_2$Cl$_2$/CH$_3$OH = 10:1) to give **14** (36.82%; m.p. 168–170 °C), **15** (36.17%; m.p. 165–167 °C), **16**

(42.30%; m.p. 75–77 °C) as white crystals, and **17** (4.2 mg; 4.05%) as transparent yellow oil.

3.4.1. 1-[2-(2-amino-3,4-bis-benzyloxy-5-oxo-2,5-dihydro-furan-2-yl)-ethyl]-1H-pyrimidine-2,4-dione (14)

^{1}H NMR (DMSO-d_6): δ 1.96 (H-5, 2H, m), 3.64 (H-6, 2H, dd, J_1 = 6.20, J_2 = 13.71), 5.01 (O$\underline{C}$H$_2$-2, 2H, s), 5.14 (O$\underline{C}$H$_2$-3, 2H, dd, J_1 = 11.91, J_2 = 22.41), 5.51 (H-6′, 1H, dd, J_1 = 1.68, J_2 = 7.77), 6.16/8.17 (NH$_2$-4, 2 × 1H, s), 7.33–7.42 (Ph, 10H, m), 7.45 (H-5′, 1H, d, J = 7.86), 11.21 (NH, 1H, s).

^{13}C NMR (DMSO-d_6): δ 35.93 (C-5), 44.01 (C-6), 72.57 (O$\underline{C}$H$_2$-2), 73.75 (O$\underline{C}$H$_2$-3), 82.22 (C-4), 101.31 (C-5′), 123.59 (C-2), 128.12–129.03 ($\underline{C}_6$H$_5$), 136.85 (C-2a), 137.25 (C-3a), 146.13 (C-6′), 151.28 (C-2′), 153.84 (C-3), 164.21 (C-4′), 168.37 (C-1). MS m/z 432.2 [M − NH$_3$]$^+$.

3.4.2. 1-[2-(2-amino-3,4-bis-benzyloxy-5-oxo-2,5-dihydro-furan-2-yl)-ethyl]-5-fluoro-1H-pyrimidine-2,4-dione (15)

^{1}H NMR (DMSO-d_6): δ 1.93–2.08 (H-5, 2H, m), 3.58–3.72 (H-6, 2H, m), 5.01 (O$\underline{C}$H$_2$-2, 2H, s), 5.14 (O$\underline{C}$H$_2$-3, 2H, dd, J_1 = 11.87, J_2 = 39.36), 6.17/8.16 (NH$_2$-4, 2 × 1H, s), 7.31–7.41 (Ph, 10H, m), 7.91 (H-6′, 1H, d, J = 3.39), 11.73 (NH, 1H, s).

^{13}C NMR (DMSO-d_6): δ 35.17 (C-5), 43.72 (C-6), 72.08 (O$\underline{C}$H$_2$-2), 73.29 (O$\underline{C}$H$_2$-3), 81.75 (C-4), 123.15 (C-2), 127.58–128.48 ($\underline{C}_6$H$_5$), 130.21 (C-6′, J_{CF} = 33.37), 136.34 (C-2a), 136.76 (C-3a), 139.39 (C-5′, J_{CF} = 228.94), 149.41 (C-3), 153.39 (C-2′), 157.41 (C-4′, J_{CF} = 25.43), 167.86 (C-1). MS m/z 466.4 [M − 1].

3.4.3. 1-[2-(2-amino-3,4-bis-benzyloxy-5-oxo-2,5-dihydro-furan-2-yl)-ethyl]-5-methyl-1H-pyrimidine-2,4-dione (16)

^{1}H NMR (DMSO-d_6): δ 1.72 (CH$_3$, 3H, s), 1.86–2.03 (H-5, 2H, m), 3.52–3.66 (H-6, 2H, m), 4.99 (O$\underline{C}$H$_2$-2, 2H, s), 5.11 (O$\underline{C}$H$_2$-3, 2H, dd, J_1 = 11.89, J_2 = 24.01), 6.13/8.13 (NH$_2$-4, 2 × 1H, 2xs), 7.27–7.40 (Ph + H-6′, 11H, m), 11.19 (NH, 1H, s).

^{13}C NMR (DMSO-d_6): δ 12.38 (CH$_3$), 35.96 (C-5), 43.66 (C-6), 72.54 (O$\underline{C}$H$_2$-2), 73.77 (O$\underline{C}$H$_2$-3), 82.21 (C-4), 108.88 (C-5′), 123.66 (C-2), 128.09–128.99 ($\underline{C}_6$H$_5$), 136.85 (C-2a′), 137.28 (C-3a′), 141.87 (C-6′), 151.21 (C-2′), 153.79 (C-3), 164.75 (C-4′), 168.37 (C-1). MS m/z 446.1 [M − NH$_3$]$^+$.

3.4.4. 2-[2-(2-amino-3,4-bis-benzyloxy-5-oxo-2,5-dihydro-furan-2-yl)-ethyl]-2H-[1,2,4]triazine-3,5-dione (17)

^{1}H NMR (DMSO-d_6): δ 1.94–2.08 (H-5, 2H, m), 3.82–3.92 (H-6, 2H, m), 5.03 (O$\underline{C}$H$_2$-2, 2H, s), 5.15 (O$\underline{C}$H$_2$-3, 2H, dd, J_1 = 11.94,

$J_2 = 41.12$), 6.14/8.12 (NH_2-4, 2 × 1H, s), 7.20–7.46 (Ph, 10H, m), 7.46 (H-5′, 1H, s), 12.08 (NH, 1H, s).
^{13}C NMR (DMSO-d_6): δ 34.32 (C-5), 45.40 (C-6), 71.54 (O$\underline{C}H_2$-2), 72.75 (O$\underline{C}H_2$-3), 81.65 (C-4), 122.74 (C-2), 127.22–133.18 ($\underline{C}_6H_5$), 134.56 (C-5′), 134.96 (C-2′), 135.84 (C-2a), 136.29 (C-3a), 153.08 (C-3), 169.12 (C-1), 169.37 (C-4′). MS m/z 451.2 [M + 1].

3.4.5. 2-[2-(3,4-bis-benzyloxy-5-oxo-2,5-dihydro-furan-2-yl)-2-hydroxy-ethyl]-2H-[1,2,4]triazine-3,5-dione (18)

Reaction of 6-azauracil (230 mg; 2.02 mmol) and **EdBA** (200 mg; 0.59 mmol) as described in method C yielded yellow oil. Crude product was purified by silica gel column chromatography (CH_2Cl_2/CH_3OH = 20:1) to give **18** (12.6 mg; 4.73%) as yellow oil.
^{13}C NMR (DMSO-d_6): δ 52.48 (C-6), 64.98 (C-5), 72.70 (O$\underline{C}H_2$-2), 73.52 (O$\underline{C}H_2$-3), 75.16 (C-4), 107.57 (C-5′), 120.57 (C-2), 127.74–128.75 ($\underline{C}_6H_5$), 135.61 (C-2a), 136.10 (C-3a), 148.46 (C-3), 157.18 (C-2′), 157.57 (C-4′), 169.14 (C-1). MS m/z 452.1 [M + 1].

3.4.6. 1-[2-(3,4-bis-benzyloxy-5-oxo-5H-furan-2-ylidene)-ethyl]-[1,3,5]triazinane-2,4,6-trione (19)

Reaction of cyanuric acid (1.5 g; 11.57 mmol) and **dAdBA** as described by method A afforded yellow oil as a crude product. Silica gel column chromatography (petrol ether/EtOAc = 2:1) yielded **19** as white crystals (172 mg; 96.26%; m.p. 128–130 °C).
^{13}C NMR (DMSO-d_6): δ 36.50 (C-6), 73.45 (O$\underline{C}H_2$-2), 74.48 (O$\underline{C}H_2$-3), 104.96 (C-5), 123.07 (C-2), 128.47–129.35 ($\underline{C}_6H_5$), 135.89 (C-2a), 136.25 (C-3a), 144.67 (C-3), 148.72 (C-4), 149.07 (C-4′), 150.10 (C-2′), 150.10 (C-6′), 164.27 (C-1). MS m/z 450.1 [M + 1].

3.4.7. 1-[2-(3,4-dihydroxy-5-oxo-5H-furan-2-ylidene)-ethyl]-[1,3,5]triazinane-2,4,6-trione (20)

Compound **19** (170 mg; 0.38 mmol) was dissolved in dry CH_2Cl_2 as per described in method D the crude product was submitted to silica gel column chromatography (CH_2Cl_2/CH_3OH = 10:1) to afford **20** as white crystals (11.4 mg; 11.15%; m.p. 184–187 °C).
^{13}C NMR (DMSO-d_6): δ 35.94 (C-6), 100.79 (C-5), 121.13 (C-2), 143.27 (C-3), 143.45 (C-4′), 148.55 (C-4), 149.58 (C-2′), 149.58 (C-6′), 164.80 (C-1). MS m/z 270.1 [M + 1].

3.4.8. 1-[2-(2-amino-3,4-bis-benzyloxy-5-oxo-2,5-dihydro-furan-2-yl)-ethyl]-[1,3,5]triazinane-2,4,6-trione (21)

To a solution of **19** (150 mg; 0.32 mmol) in methanol (15 mL) and dioxane (10 mL) ammonia was introduced as described in method B. The crude product was purified by silica gel column chromatography (CH_2Cl_2/CH_3OH = 10:1) to give **21** as colorless oil (21.3 mg; 13.84%).
^{13}C NMR (DMSO-d_6): δ 36.54 (C-6), 72.55 (O$\underline{C}H_2$-2), 73.78 (O$\underline{C}H_2$-3), 82.29 (C-5), 123.63 (C-2), 128.12–129.13 ($\underline{C}_6H_5$), 136.89 (C-2a), 137.25 (C-3a), 149.14 (C-3), 150.19 (C-2′), 150.19 (C-6′), 150.39 (C-4′), 153.77 (C-4), 168.26 (C-1). MS m/z 467.2 [M + 1].

3.4.9. 1-[2-(3,4-bis-benzyloxy-5-oxo-2,5-dihydro-furan-2-yl)-2-hydroxy-ethyl]-[1,3,5]triazinane-2,4,6-trione (22)

Reaction of cyanuric acid (260 mg; 2.01 mmol) and **EdBA** (200 mg; 0.59 mmol) as described in method C gave crude product in the form of yellow oil that was submitted to silica gel column chromatography (CH_2Cl_2/CH_3OH = 50:1) to afford **22** as yellow oil (36.7 mg; 13.31%).
^{13}C NMR (DMSO-d_6): δ 44.60 (C-6), 66.27 (C-5), 72.71 (O$\underline{C}H_2$-2), 73.53 (O$\underline{C}H_2$-3), 120.43 (C-2), 127.87–129.15 ($\underline{C}_6H_5$), 135.58 (C-2a), 136.47 (C-3a), 142.06 (C-2′), 146.14 (C-4′), 150.94 (C-6′), 156.93 (C-3), 167.67 (C-1). MS m/z 468.1 [M + 1].

3.5. X-ray crystal structure determination of 13

The crystal suitable for X-ray single crystal structure study was grown by slow evaporation from ethanol solution at room temperature. Data were collected on a Bruker-Nonius Kappa Apex II diffractometer using graphite-monochromated Cu$K\alpha$ radiation (λ = 1.54184 Å) at 123 K. COLLECT [36] software was used for the data collection and DENZO-SMN [37] for data processing. The intensities were corrected for absorption using the SADABS2008 [38]. The crystal structure was solved by direct methods [39] and all non-hydrogen atoms were refined anisotropically by full-matrix least squares calculations based on F^2 [40] using the programs integrated in WinGX program package [41]. The hydrogen atom attached to the N3 atom was found in a difference Fourier map and was refined isotropically. All other hydrogen atoms were treated using appropriate riding models, with SHELXL97 [40] defaults. PLATON [42] program was used for structure analysis and drawings preparation. Crystallographic data for the structure reported in this paper have been deposited with the Cambridge Crystallographic Data Centre. These data can be obtained free of charge from The Cambridge Crystallographic Data Centre via www.ccdc.cam.ac.uk/data_request/cif.

Crystal data for **13**: crystal dimension 0.15 × 0.20 × 0.60 mm^3 (colourless prism); $C_{23}H_{19}N_3O_6$, M_r = 433.41, monoclinic space group P 2$_1$/c (No. 14); a = 9.8162(9), b = 23.191(2), c = 9.1177(7) Å, β = 95.206(5)o; V = 2067.1(3) Å^3; Z = 4; d_x = 1.393 g cm^{-3}; μ(Cu Kα) = 0.856 mm^{-1}; 14087 reflections measured, R/wR = 0.0740/0.1788 for 294 parameters and 2146 reflections with $I \geq 2\sigma(I)$, R/wR = 0.1147/0.2092 for all 3338 unique reflections measured in the range 7.62°– 2θ –126.54°; S = 0.961.

3.6. Cell culturing

The cell lines HeLa (cervical carcinoma), SW620 (colorectal adenocarcinoma, metastatic), MiaPaCa-2 (pancreatic carcinoma), MCF-7 (breast epithelial adenocarcinoma, metastatic), HepG2 (hepatocellular carcinoma) and WI 38 (normal diploid human fibroblasts), were cultured as monolayers and maintained in Dulbecco's modified Eagle medium (DMEM) supplemented with 10% fetal bovine serum (FBS), 2 mM L-glutamine, 100 U/ml penicillin and 100 μg/mL streptomycin in a humidified atmosphere with 5% CO_2 at 37 °C.

3.7. Proliferation assays

The panel cell lines were inoculated onto a series of standard 96-well microtiter plates on day 0, at 3000 cells to 6000 cells per well according to the doubling times of specific cell line. Test agents were then added in five, 10-fold dilutions (0.01–100 μM) and incubated for further 72 h. Working dilutions were freshly prepared on the day of testing in the growth medium. The solvent (DMSO) was also tested for eventual inhibitory activity by adjusting its concentration to be the same as in the working concentrations (DMSO concentration never exceeded 0.1%). After 72 h of incubation, the cell growth rate was evaluated by performing the MTT assay: experimentally determined absorbance values were transformed into a cell percentage growth (PG) using the formulas proposed by NIH and described previously [43]. This method directly relies on control cells behaving normally at the day of assay because it compares the growth of treated cells with the growth of untreated cells in control wells on the same plate – the results are therefore a percentile difference from the calculated expected value.

The IC$_{50}$ values for each compound were calculated from dose-response curves using linear regression analysis by fitting the mean test concentrations that give PG values above and below the reference value. If, however, all of the tested concentrations produce PGs exceeding the respective reference level of effect (e.g. PG value of 50) for a given cell line, the highest tested concentration is assigned as the default value (in the screening data report that default value is preceded by a ">" sign). Each test point was

performed in quadruplicate in three individual experiments. The results were statistically analyzed (ANOVA, Tukey post-hoc test at $p < 0.05$). Finally, the effects of the tested substances were evaluated by plotting the mean percentage growth for each cell type in comparison to control on dose-response graphs.

3.8. DNA cell cycle analysis

Flow cytometric analysis was used to measure the DNA content of the cells. Briefly, 3×10^5 cells were seeded per well in 6-well plates. After an overnight incubation, compounds **1** (5 μM and 10 μM) and **2** (1 μM and 5 μM) were added, and the cells were cultured for 24 and 48 h. The cells were then harvested by trypsinization, washed three times with phosphate buffered saline (PBS), fixed with cold ethanol and stored at −20 °C. Immediately before analysis, cell suspension was centrifuged, the pellet was washed twice with PBS and incubated with 0.2 μg/μL RNase A at 37 °C for 15 min, followed by staining with propidium iodide (PI) at 10 μg/mL final concentration for 30 min in the dark. Analysis was carried out using FACScalibur instrument (BD Biosciences, San Jose, CA), whereby approximately 20,000 events were recorded for each sample. WinMDI 2.8 (The Scripps Institute, La Jolla, CA) and Cylchred (Cardiff University, Cardiff, UK) software were used to determine the percentage of the cells in different phases of the cell cycle.

3.9. Annexin V test

Detection and quantification of apoptotic cells at single cell level were performed using Annexin V-FLUOS staining kit (e-Bioscience) according to the manufacturer's instructions. Briefly, MCF-7, HeLa, MiaPaCa-2 and SW620 cells were seeded in 6-well plates (1×10^5 cells/well), incubated for 24 h and treated with compounds **1** (5 μM and 10 μM) and **2** (1 μM and 5 μM). After 24 and 48 h, the slides were washed with PBS and with manufacturer's binding buffer, incubated with annexin-V for 10 min, washed with binding buffer and incubated with PI. Slides were observed under the Olympus epifluorescent microscope to examine the cells for their content of viable and apoptotic/necrotic populations.

4. Conclusions

A series of novel cytosine derivatives containing $C4$-$C5$ double bond conjugated with the lactone moiety (**1–4**, **13**, **19**, **20**) and their congeners bearing free hydroxy group at C-5 of ethylenic spacer (**7–9**, **18**, **22**), as well as pyrimidine derivatives (**5**, **6**, **14–17**, **21**) with the amino group at the C-4 of the lactone moiety were synthesized and evaluated for their cytostatic activity against malignant human tumour cell lines. In general, tested compounds showed modest and non-specific antiproliferative effects. However, the cytosine derivative of L-ascorbic acid containing $C4$-$C5$ double bond (**1**) produced rather marked growth inhibitory effects on HepG2, MCF-7 and HeLa cell lines, as well as significant cytotoxic effect on human normal fibroblasts. However, the most potent antitumour activity was observed with 5-azacytosine derivative of L-ascorbic acid with a double bond at the $C4$–$C5$ conjugated with the lactone moiety (compound **2**), especially in MiaPaCa-2, HepG2 and MCF-7 cells. This compound however, showed non-selective (SI = 5.07) antitumour activity compared to normal human fibroblasts. Flow cytometric analysis of the cell cycle revealed significant and rather specific effect of this compound on the cell cycle progression of MiaPaCa-2, SW620 and HeLa cell lines triggering S-phase arrest with concomitant reduction in G1 phase cell population. This nucleic acid antimetabolite activity might be attributable to the structural similarity of compound **2** with nucleotides.

Comparison of the CD spectra of **7** and **8** with their synthetic precursor 4-(5,6)-epoxy derivative of L-ascorbic acid (**EdBA**, Scheme 1) permitted to deduce their absolute configuration. Thus, the derivatives with the hydroxy group at the C-5 of ethylenic spacer (**7**, Fig. 2B and **8**, Fig. 2A) exist in 4R, 5S enantiomeric form. This means that the ring-opening reaction step (Schemes 2 and 3) proceeds in enantiospecific manner with the retention of configuration.

On the other hand, derivatives of L-ascorbic acid with the free amino group at the C-4 of the lactone moiety (**5**, **6**, **14–17** and **21**), in general, do not show Cotton effect supporting the assumption that the attack goes equally from both sides of the $C4$–$C5$ double bond resulting in racemic mixtures of enantiomers.

X-ray crystal structure study of 6-azauracil derivative of L-ascorbic acid **13** confirms the Z-configuration of the double bond. Both benzyloxy groups adopt the same, antiperiplanar conformation. One N−H⋯O hydrogen bond, two C−H⋯O hydrogen bonds and two C−H⋯π interactions self-assemble the molecules into three-dimensional framework.

References

[1] A. Matsuda, K. Takenuki, T. Sasaki, T. Ueda, J. Med. Chem. 34 (1991) 812.
[2] W. Plunkett, P. Huang, Y.Z. Xu, V. Heinemann, R. Grunewald, V. Gandhi, Semin. Oncol. 22 (1995) 3.
[3] A. Azuma, K. Hanaoka, A. Kurihara, T. Kobayashi, S. Miyaushi, N. Kamo, M. Tanaka, T. Sasaki, A. Matsuda, J. Med. Chem. 38 (1995) 3391.
[4] E. Cameron, L. Pauling, Oncology 27 (1973) 181.
[5] G. Block, Am. J. Clin. Nutr. 53 (1991) 270S.
[6] B. Frei, Am. J. Med. 97 (1994) 5S.
[7] S. Uddin, S. Ahmad, Comprehen. Therap. 21 (1995) 41.
[8] C.S. Thao, Am. J. Clin. Nutr. 54 (1991) 1274S.
[9] C.H. Park, B.F. Kimler, Am. J. Clin. Nutr. 54 (1991) 1241S.
[10] M. Eckert-Maksić, I. Kovaček, Z.B. Maksić, M. Osmak, K. Pavelić, in: Z.B. Maksić, M. Eckert-Maksić (Eds.), Molecules in Natural Science and Medicine. An Encomium for Linus Pauling, Ellis Horwood, New York, 1991, pp. 509–524.
[11] K. Murakami, N. Muto, G.K. Fukasawa, I. Yamamoto, Biochem. Pharmacol. 44 (1992) 2191.
[12] M.W. Roomi, D. House, M. Eckert-Maksić, Z.B. Maksić, C.S. Tsao, Cancer Lett. 122 (1998) 93.
[13] K. Pavelić, Brain Res. 342 (1985) 369.
[14] M.A. Medina, R.G. Veas, L. Schweigerer, Biochem. Mol. Biol. Inter. 34 (1994) 871.
[15] M.W. Roomi, D. House, C.S. Tsao, Cancer Biochem. Biophys. 16 (1998) 295.
[16] W.A. Banks, A.J. Kastin, Brain Res. Bull. 15 (1985) 287.
[17] A.K. Naidu, M. Wiranowska, S.H. Kori, L.D. Prockop, A.P. Kulkarni, Anticancer Res. 13 (1993) 1469.
[18] A.K. Naidu, M. Wiranowska, S.H. Kori, L.D. Prockop, A.P. Kulkarni, J. Neuro-Oncol. 16 (1993) 1.
[19] Y. Makino, H. Sakagami, M. Takeda, Anticancer Res. 19 (1999) 3125.
[20] H. Ashino, M. Shimamura, H. Nakajima, M. Dombou, S. Kawanaka, T. Oikawa, T. Iwaguchi, S. Kawashima, Angiogenesis 6 (2003) 259.
[21] T. Gazivoda, M. Plevnik, J. Plavec, S. Kraljević, M. Kralj, K. Pavelić, J. Balzarini, E. De Clercq, M. Mintas, S. Raić-Malić, Bioorg. Med. Chem. 13 (2005) 131.
[22] S. Raić-Malić, D. Svedružić, T. Gazivoda, A. Marunović, A. Hergold-Brundić, A. Nagl, J. Balzarini, E. De Clercq, M. Mintas, J. Med. Chem. 43 (2000) 4806.
[23] S. Raić-Malić, A. Hergold-Brundić, A. Nagl, M. Grdiša, K. Pavelić, E. De Clercq, M. Mintas, J. Med. Chem. 42 (1999) 2673.
[24] G. Snatzke, L. Hruban, F. Snatzke, Isr. J. Chem. 15 (1976/77) 46.
[25] K. Pál, M. Kállay, M. Kubinyi, P. Bakó, A. Makó, Tetrahedron Asymmetry 18 (2007) 1521.
[26] B. Ringdahl, Acta Scand. B. 38 (1983) 141.
[27] W.C. Kreuger, R.A. Johnson, L.M. Psichoda, J. Am.Chem. Soc. 93 (1971) 4865.
[28] H. Suzuki, Electronic Absorption Spectra and Geometry of Organic Molecules. Academic, New York, 1967, p. 463.
[29] K. Wittine, T. Gazivoda, M. Markuš, D. Mrvoš-Sermek, A. Hergold-Brundić, M. Cetina, D. Žiher, V. Gabelica, M. Mintas, S. Raić-Malić, J Mol. Struct. 687 (2004) 101.
[30] J.K. Christman, Oncogene 21 (35) (2002) 5483–5495.
[31] J. Vesely, A. Cihak, Pharmac. Ther. A. 2 (1978) 813–840.

[32] J.K. Christman, N. Mendelsohn, D. Herzog, N. Schneiderman, Cancer Res. 43 (1983) 763–769.

[33] L. Jackson-Grusby, P.W. Laird, S.N. Magge, B.J. Moeller, R. Jaenisch, Proc. Natl. Acad. Sci. U. S. A. 94 (1997) 4681–4685.

[34] J.I. Johnson, S. Decker, D. Zaharevitz, L.V. Rubinstein, J.M. Venditti, S. Schepartz, S. Kalyandrug, M. Christian, S. Arbuck, M. Hollingshead, E.A. Sausville, Br. J. Cancer 84 (2001) 1424–1431.

[35] T. Voskoglou-Nomikos, J.L. Pater, L. Seymour, Clin. Cancer Res. 9 (2003) 4227.

[36] R.W.W. Hooft, Collect. Nonius BV, Delft, The Netherlands, 1998.

[37] Z. Otwinowski, W. Minor, Processing of X-ray diffraction data collected in oscillation mode. in: C.W. CarterJr., R.M. Sweet (Eds.), Methods in Enzymology, Macromolecular Crystallography, Part A, vol. 276. Academic Press, New York, 1997, pp. 307–326.

[38] G.M. Sheldrick, SADABS 2008/2. University of Göttingen, Göttingen, Germany, 2008.

[39] M.C. Burla, M. Camalli, B. Carrozzini, G.L. Cascarano, C. Giacovazzo, G. Polidori, R. Spagna, J. Appl. Crystallogr. 36 (2003) 1103.

[40] G.M. Sheldrick, Acta Crystallogr. A64 (2008) 112.

[41] L.J. Farrugia, J. Appl. Cryst. 32 (1999) 837.

[42] A.L. Spek, J. Appl. Crystallogr. 36 (2003) 7.

[43] T. Gazivoda, S. Raić-Malić, V. Krištafor, D. Makuc, J. Plavec, S. Bratulić, S. Kraljević-Pavelić, K. Pavelić, L. Naesens, G. Andrei, R. Snoeck, J. Balzarini, Mintas Bioorg. Med. Chem. 16 (2008) 5624.